CUKUROVA UNIVERSITY
INSTITUTE OF NATURAL AND APPLIED SCIENCES

MSc THESIS

Analysis of The Brain's Network Based on Electroencephalograms and Classification of Movement Events Using Connectivity Maps and Features

Salih MENDİ

Electrical and Electronics Engineering Department

January, 2025

CUKUROVA UNIVERSITY
INSTITUTE OF NATURAL AND APPLIED SCIENCES

MSc THESIS APPROVAL

Analysis of The Brain's Network Based on Electroencephalograms and Classification of Movement Events Using Connectivity Maps and Features

Salih MENDİ

Electrical and Electronics Engineering Department

This Master's Thesis was evaluated by the following Jury Members on …/.../…… and was approved by unanimity / majority of votes.

Jury :Assoc. Prof. Dr. Ahmet Aydın (Advisor) …………

: Assist. Prof. Dr. Oğuzhan TİMUR …………

: Assoc. Prof. Dr. Kutlucan GÖRÜR …………

This Thesis was written in the Department of Electrical and Electronics Engineering, Institute of Natural and Applied Sciences.

Thesis Number:

Prof. Dr. Sadık DİNÇER
Director
Institute of Natural and Applied Sciences

Note: The usage of the presented specific declarations, tables, figures, and photographs either in this thesis or in any other reference without citation is subject to "The law of Arts and Intellectual Products" number of 5846 of Turkish Republic

CONTENTS

CUKUROVA UNIVERSITY
INSTITUTE OF NATURAL AND APPLIED SCIENCES

MSc THESIS

Analysis of The Brain's Network Based on Electroencephalograms and Classification of Movement Events Using Connectivity Maps and Features

Salih MENDİ

Advisor: Assoc. Prof. Dr. Ahmet Aydın

Department of Electrical and Electronics Engineering

ABSTRACT

The brain-computer interface (BCI) is a technology that allows individuals with physical disabilities to communicate and interact with the external environment using brain signals. One of the key applications of BCI is motor imagery (MI), where an individual imagines performing a movement, and the corresponding brain activity is captured through electroencephalogram (EEG) signals. MI based BCI systems have attracted considerable attention due to their potential to facilitate movement recovery and control of external devices solely through brain activity. In this study, a novel approach is presented for feature extraction and classification of EEG signals recorded during motor imagery tasks. Features were extracted using the correlation coefficient and covariance matrices. These features were subsequently classified using three different machine learning models, which are Feed Forward Neural Network (FFNN), Naive Bayes Classifier (NBC), and Linear Discriminant Analysis (LDA) Classifier. The proposed method was validated on Dataset 2a of BCI Competition IV, which includes EEG data from four distinct motor imagery categories: left hand, right hand, both feet, and tongue movements. The comparative analysis showed that the features derived from the covariance matrix consistently exceeded those based on the correlation coefficient matrix across all classifiers. In particular, the covariance matrix features achieved the highest classification accuracy. Thus, they demonstrated outstanding performance in terms of robustness and reliability in the classification of different motor imagery tasks. The results of this study highlight the effectiveness of covariance matrix based feature extraction methods for MI based BCI systems, providing a promising way to improve classification accuracy and system performance. This advancement holds significant potential for real world BCI applications, such as restoring motor function to paralyzed individuals, improving the quality of life for people with disabilities, and facilitating seamless human computer interaction in virtual and augmented reality environments. By leveraging the brain's neural activity, this approach can enable paralyzed individuals to regain a degree of autonomy and contribute to the broader development of assistive technologies and immersive interfaces.

Keywords: Brain computer interface (BCI), Motor imagery (MI), Correlation, Covariance, Electroencephalogram (EEG).

ÇUKUROVA ÜNİVERSİTESİ
FEN BİLİMLERİ ENSTİTÜSÜ

YÜKSEK LİSANS TEZİ

Elektroensefalogramlara Dayalı Beyin Ağı Analizi ve Hareket Olaylarının Bağlantı Haritaları ve Özellikler Kullanılarak Sınıflandırılması

Salih MENDİ

Danışman: Doç. Dr. Ahmet Aydın

Elektrik Elektronik Mühendisliği Anabilim Dalı

ÖZ

Beyin-bilgisayar arayüzü (BBA), fiziksel engelli bireylerin beyin sinyallerini kullanarak dış çevre ile iletişim ve etkileşim kurmasını sağlayan bir teknolojidir. BCI'ın temel uygulamalarından biri, bireyin bir hareketi gerçekleştirdiğini hayal ettiği ve ilgili beyin aktivitesinin elektroensefalogram (EEG) sinyalleri aracılığıyla yakalandığı motor imgelemedir (MI). MI tabanlı BCI sistemleri, yalnızca beyin aktivitesi yoluyla hareket ve harici cihazların kontrolünü kolaylaştırma potansiyelleri nedeniyle büyük ilgi görmüştür. Bu çalışmada, motor imgeleme görevleri sırasında kaydedilen EEG sinyallerinin özellik çıkarımı ve sınıflandırılması için yeni bir yaklaşım sunulmuştur. Özellikler korelasyon katsayısı ve kovaryans matrisleri kullanılarak çıkarılmıştır. Bu özellikler daha sonra İleri Beslemeli Yapay Sinir Ağı, Naive Bayes Sınıflandırıcı ve Lineer Diskriminant Analizi Sınıflandırıcı olmak üzere üç farklı makine öğrenimi modeli kullanılarak sınıflandırılmıştır. Önerilen yöntem, sol el, sağ el, her iki ayak ve dil hareketleri olmak üzere dört farklı MI kategorisinden EEG verilerini içeren BCI Competition IV'ün Veri Kümesi 2a üzerinde doğrulanmıştır. Karşılaştırmalı analiz, kovaryans matrisinden türetilen özelliklerin, tüm sınıflandırıcılar arasında korelasyon katsayısı matrisine dayalı olanları tutarlı bir şekilde aştığını göstermiştir. Özellikle, kovaryans matris özellikleri en yüksek sınıflandırma doğruluğuna ulaşmıştır. Böylece, farklı MI görevlerinin sınıflandırılmasında sağlamlık ve güvenilirlik açısından üstün performans göstermişlerdir. Bu çalışmanın sonuçları, MI tabanlı BCI sistemleri için kovaryans matris tabanlı özellik çıkarma yöntemlerinin etkinliğini vurgulamakta ve sınıflandırma doğruluğunu ve sistem performansını iyileştirmek için umut verici bir yol sağlamaktadır. Bu ilerleme, felçli bireylere motor fonksiyonlarını geri kazandırmak, engelli insanların yaşam kalitesini artırmak ve sanal ve artırılmış gerçeklik ortamlarında sorunsuz insan bilgisayar etkileşimini kolaylaştırmak gibi gerçek dünya BBA uygulamaları için önemli bir potansiyele sahiptir. Bu yaklaşım, beynin sinirsel aktivitesinden yararlanarak felçli bireylerin bir dereceye kadar özerklik kazanmasını sağlayabilir ve yardımcı teknolojilerin ve sürükleyici arayüzlerin daha geniş çapta geliştirilmesine katkıda bulunabilir.

Anahtar Kelimeler:Beyin bilgisayar arayüzü (BBA), Motor İmgeleme (MI), Korelasyon, Kovaryans, Elektroensefalogram (EEG).

GENİŞLETİLMİŞ ÖZET

Elektroensefalogramlara Dayalı Beyin Ağı Analizi ve Hareket Olaylarının Bağlantı Haritaları ve Özellikler Kullanılarak Sınıflandırılması

Beyin-bilgisayar arayüzü (BBA), beynin elektriksel aktivitesi ile bilgisayar veya protez uzuv gibi harici bir cihaz arasında doğrudan bir iletişim yolu sağlayan bir teknolojidir. Bu teknoloji, makinelerle etkileşim kurma şeklimizde devrim yaratma potansiyeline sahiptir. Örneğin, BBA'lar felçli bireylerin bilgisayarları veya protez uzuvları düşünceleriyle kontrol etmelerine yardımcı olabilir. Ayrıca, epilepsi de dahil olmak üzere çeşitli bozuklukların tespit ve teşhisine yardımcı olabilirler.

Üç tür BBA vardır: noninvaziv, invaziv ve kısmen invaziv. Invaziv BBA'lar, elektrotları doğrudan beyne implante etmek için ameliyat gerektirir, bu da en yüksek kalitede sinyal sağlayabilir, ancak aynı zamanda en büyük enfeksiyon ve diğer komplikasyon riskini de taşır. Noninvaziv BBA'lar beyin aktivitesini ölçmek için kafa derisine yerleştirilen elektrotları kullanır ve invaziv BBA'lardan daha güvenlidir ancak daha az doğru olabilir. Kısmen invaziv BBA'lar kafatasının içine implante edilir, cihazın geri kalanı beynin dışındadır, bu da noninvaziv BBA'lardan daha iyi sinyal çözünürlüğü sağlar.

Genel olarak beyin-bilgisayar arayüzü (BBA), elektroensefalografi (EEG) sinyallerini kullanarak insan beyni ile bilgisayar gibi makineler arasında bir iletişim aracıdır. Daha fazla araştırma ve geliştirme ile BBA'lar, engelli ve diğer tıbbi rahatsızlıkları olan bireylerin yaşamlarını büyük ölçüde iyileştirme potansiyeline sahiptir.

EEG sinyallerinin incelenmesi 20. yüzyılın başlarına kadar uzanmaktadır. 1929 yılında Hans Berger, beyin dokusu nöronlarının elektriksel aktivitesinin bir yorumunu sunarak EEG araştırmalarının ve modern sinir biliminin başlangıcını oluşturdu.

Elektroensefalogram (EEG), beynin elektriksel özelliklerini ölçmek için değerli ve benzersiz bir yöntemdir. Beyin aktivitesini kaydetmek için en çok kullanılan noninvaziv tekniktir ve basitliği ve düşük maliyeti nedeniyle birçok noninvaziv BCI sisteminde yaygın olarak kullanılmaktadır.

Bir EEG sinyali, uyarıldıklarında serebral korteksteki birçok piramidal nöronun dendritlerinden akan elektrik akımlarını ölçer. Bu akımlar Elektromiyogram (EMG) ekipmanı tarafından ölçülebilen bir manyetik alan yaratır. EEG sistemi ise kafa derisi boyunca oluşan ikincil elektrik alanını ölçer.

Beyindeki elektrik potansiyellerindeki farklılıklar, piramidal hücrelerden gelen kademeli potansiyellerin birleşik etkileri tarafından oluşturulur. Bu kademeli potansiyeller soma (bir nöronun gövdesi) ile nöronlardan dallanan apikal dendritler arasında elektrik dipollerine neden olur. Beyindeki akım esas olarak sodyum (Na^+), potasyum (K^+), kalsiyum (Ca^{++}) gibi pozitif iyonların ve klor (Cl^-) gibi negatif iyonların nöron membranlarından membran potansiyeli tarafından belirlenen yönde pompalanmasıyla üretilir.

Bir nöron uyarıldığında, membran potansiyeli değişir ve bu da bir aksiyon potansiyelini tetikleyebilir. Bu, nöronun aksonundan aşağıya doğru ilerleyen kısa bir elektriksel aktivite dalgasıdır. Beyinde, nöron grupları genellikle senkronize olarak birlikte ateşlenir ve EEG elektrotlarının tespit edebileceği elektrik akımları üretir. EEG sinyali, bu senkronize nöron popülasyonlarının toplam elektriksel aktivitesini yansıtır ve çeşitli frekans ve genliklere sahip karmaşık bir dalga biçimidir. Sinyaldeki farklı frekanslar farklı beyin durumlarıyla ilişkilidir

EEG sinyali rastgele bir elektriksel aktivite koleksiyonu değildir. Bunun yerine, frekans aralıklarına göre farklı bantlarda sınıflandırılan farklı frekanslarda ritmik aktivite sergiler. Delta dalgaları (0,1-4 Hz) derin uyku ile ilişkilendirilirken, teta dalgaları (4-8 Hz) uyuşukluk, uykunun erken evresi ve hayal kurma ile bağlantılıdır. Alfa dalgaları (8-12 Hz) rahat ama uyanık bir zihinle ilişkilidir ve bir kişi gözlerini kapattığında veya sessizce dinlendiğinde öne çıkarlar. Beta dalgaları (13-30 Hz) aktif uyanıklık, odaklanmış dikkat ve problem çözme ile bağlantılıdır. Son olarak, gama dalgaları (30-100 Hz) yüksek frekanslı dalgalardır ve algılama, öğrenme ve hafıza gibi üst düzey bilişsel işlevlerle ilişkilidir.

Motor imgeleme, herhangi bir fiziksel hareket olmaksızın zihinsel olarak bir motor eylemi gerçekleştirme uygulamasıdır. Bir hareketin zihinde canlandırılması sırasında benzer beyin bölgelerinin ve işlevlerinin kullanıldığı genel olarak kabul edilmektedir. Motor imgeleme (MI), oyun endüstrisi de dahil olmak üzere beyin-bilgisayar arayüzü (BBA) uygulamalarında devrim yaratabilecek güçlü bir tekniktir.

Bu çalışmada BCI Competition IV 'ün 2a veri seti (Brunner C. et al 2008) incelenmiştir. Bu veri seti 9 denekten alınan EEG verilerinden oluşmaktadır. İşaret tabanlı BCI paradigması, sol el (sınıf 1), sağ el (sınıf 2), her iki ayak (sınıf 3) ve dil (sınıf 4) hareketinin hayal edilmesi olmak üzere dört farklı motor imgeleme görevinden oluşmuştur. Her denek için farklı günlerde iki oturum kaydedilmiştir. Her oturum kısa aralarla ayrılmış 6 çalışmadan oluşmaktadır. Bir çalışma 48 denemeden (olası dört sınıfın her biri için 12 deneme) oluşmakta ve oturum başına toplam 288 deneme elde edilmektedir. Ve her sınıf için 72 deneme kaydedilmiştir.

EEG kaydı için yirmi iki Ag/AgCl elektrot (elektrotlar arası mesafeler 3,5 cm) kullanılmıştır. Tüm sinyaller monopolar olarak kaydedilmiş, sol mastoid referans ve sağ mastoid toprak olarak kullanılmıştır. Sinyaller 250 Hz ile örneklenmiş ve 0,5 Hz ile 100 Hz arasında bant geçiren filtreden geçirilmiştir. Amplifikatörün hassasiyeti 100 μV olarak ayarlanmıştır. Hat gürültüsünü bastırmak için ek bir 50 Hz notch filtresi etkinleştirilmiştir.

Veri setinin detayları, veri setinin sahipleri tarafından sağlanan açıklama dosyasında bulunabilir.

Elektrotların yerleşimi ve elektrot sistemi göz önünde bulundurularak, elektrotlar eşlemede kullanılmak üzere aşağıdaki şekilde adlandırılmıştır:

Channel_list={'Fz','FC3','FC1','FCz','FC2','FC4','C5','C3','C1','Cz','C2','C4','C6','CP3','CP1',' CPz','CP2','CP4','P1','Pz','P2','POz'};

Sinyal işlemeler Matlab (Mathworks Inc.) ortamında yapılmıştır. Bu çalışmada veri setinin 3 ila 6 saniye arasındaki sinyale karşılık gelen Motor İmgeleme sinyali kısmı kullanılmıştır (Şekil 9). Herhangi bir veri işlenmeden önce, ham EEG verilerinin eksik örnekleri sıfırlarla doldurulmuştur. Ve veri seti, veri seti açıklama dosyasında ayrıntılı olarak açıklanan olay tipi etiketine göre kategorilere ayrılmıştır. 22 EEG kanalı verisi kullanılmış ve 3 EOG kanalı verisi hariç tutulmuştur.

Bu çalışmanın aşamaları şu şekilde detaylandırılmıştır:

Deneklerden biri ve sınıflardan biri rastgele seçilmiş (A1T- Sınıf 1) ve 22 kanal için sinyal izlenmiştir.

Sinyalin gücü ve 72 deneme olan 3. boyutun ortalaması hesaplanmıştır. Denek 1 için beyin topolojisi bu hesaplamalara göre görselleştirilmiştir.

Denek 1 için sinyaller Genel Ortalama yöntemi ile normalize edilmiş ve beyin haritalaması oluşturulmuştur.

Sinyaller her denek için ayrı ayrı periodogram hesaplamasıyla zaman düzleminden frekans düzlemine geçirilmiş ve Sinyaller bantlara ayrılmıştır. Periyodogram hesaplamasından sonra elektrotlardaki elektriksel aktiviteyi görselleştirmek için beyin haritalaması yapılmıştır.

Komşu elektrotların elektriksel aktivitesini azaltmak ve düşük frekenaslardaki sinyallerde aktif olarak kullanılan Discrete Cosine Transform (DCT) ile özellik çıkarma işlemi gerçekleştirilmiştir. Sinyaller bantlara ayrılmış ve elektrotlardaki elektriksel aktiviteyi görselleştirmek için beyin haritalaması yapılmıştır.

EEG sinyallerindeki bağımsız bileşenlerin tespit edilmesi ve bunlar sayesinde ağırlıklı matrislerin hesaplanması için Reconstruction Independent Component Analysis (rICA) kullanılmıştır. Sinyaller bantlara ayrılmış ve elektrotlardaki elektriksel aktiviteyi görselleştirmek için beyin haritalaması yapılmıştır.

Periodogram, DCT ve rICA yöntemlerinde önceden işlenmiş sinyaller, Teta, Alfa, Beta bantları için elektrotlardaki elektriksel aktiviteye göre beyin haritalama yoluyla karşılaştırılmıştır. Elde edilen sonuçlar bu özellik çıkarma fonksiyonlarının istenilen başarıyı sağlayamadığı gözlemlenlmiş ve çalışmanın bundan sonraki kısımlarında kullanılmamışlardır.

EEG elektrotlarından elde edilen sinyaller işlenerek elektrotlar kafatası iletkenliği açısından birbirleri ile korele edilmiş (Coherence hesaplanmış) ve beyin haritalaması yapılmıştır. Elde edilen sonuçlar birbirine çok yakın olduğu için çalışmanın bu yönde devam edecek kadar başarılı olmadığına karar verilmiş ve bu kafatası iletkenliği ve beyin haritalaması işlemlerine devam edilmemiştir.

Çalışmada uygulanan özellik çıkarma yöntemleri (Genel Ortalama, peridogram, DCT, rICA) ve beyin haritalama işlemleri maalesef bu yöntemler üzerinde çalışmaya devam edecek kadar başarı ile sonuçlanmamıştır.

Korelasyon katsayısı ve kovaryans matrisleri hesaplanmış ve bu matrisler temel özellik çıkarma yönlemleri olacak şekilde ek özellik çıkarma yöntemleri uygulanmıştır.

Korelasyon katsayısı ve kovaryans matrisleri hesaplanmış ve hesaplanan matrisler üzerinde ortalama, standart sapma, varyans gibi ek özellik çıkarma yöntemleri uygulanmıştır. Yeni matrisler sınıflandırma sürecine dahil edilmiştir. Sınıflandırma yöntemleri olarak İleri Beslemeli Yapay Sinir Ağı (İBYSA), Naive Bayes Sınıflandırıcı (NBS) ve Lineer Diskriminant Analizi Sınıflandırıcı (LDAS) kullanılmıştır. Hesaplamalar, deneklerin kaydedilen EEG sinyal spektrumunun sadece alfa ve beta bantları üzerinde gerçekleştirilmiştir. Hesaplamalar için sinyalin motor imgeleme kısmının 3 saniyesi kullanılmıştır. Veri setinin 0.75'i rastgele seçilen eğitim verisi olarak kullanılmış, 0.25'i ise test amacıyla seçilmiştir.

Çalışmada, ek özellik çıkarma yöntemleri olarak uygulanan Ortalama, Standart Sapma, Varyans yöntemleri sınıflandırma sonuçları istenilen başarıyı sağlayamamıştır. Bu nedenle çalışmanın sonraki safhalarında bu yöntemler kullanılmamıştır. Elde edilmiş olan en yüksek sınıflandırma doğruluğu %40 olarak gerçekleşmiştir.

Özellik çıkarma yöntemleri Ortalama, standart sapma ve varyans Relieff ile değiştirilmiş ve bir önceki adımla aynı işlemler gerçekleştirilmiştir.

Ne yazık ki, çalışmada ek özellik çıkarma olarak uygulanan ReliefF yöntemi, bu yöntem üzerinde çalışmaya devam etmek için başarı ile sonuçlanmamıştır. En yüksek sınıflandırma doğruluğu %46,45 olarak elde dilmiştir.

Özellik çıkarma yöntemi Relieff, PCA ile değiştirilmiş ve bir önceki adımla aynı işlemler gerçekleştirilmiştir. Sınıflandırma için bir önceki çalışmadan farklı olarak sadece FFNN kullanılmıştır.

Ek özellik çıkarma yöntemi PCA uygulanan veriler için sonuçlar korelasyon katsayısı ve kovaryans matrisleri ile karşılaştırıldığında, PCA uygulanan veriler için sınıflandırma doğruluğu %83,40'tır. Ancak, sadece korelasyon katsayıları ve kovaryans matrisleri hesaplanan veriler daha yüksek sınıflandırma doğruluklarına sahip olduğu gözlemlenmiştir. Bu nedenle, ek özellik çıkarımı yapılmamasına ve özellik çıkarma yöntemi olarak, korelasyon katsayısı ve kovaryans matrisleri hesaplanan veriler üzerinde daha detaylı çalışma yapılmasına karar verilmiştir.

Bu aşamaya kadar yapılan çalışmalar sonucunda korelasyon katsayısı ve kovaryans matrisleri dışındaki özellik çıkarma işlemlerinin yeterince başarılı olmadığı görülmüştür. Bu nedenle çalışmanın bundan sonraki aşamasında özellik çıkarma yöntemi olarak sadece korelasyon katsayısı ve kovaryans matrisleri kullanılmıştır. Bu aşamaya kadar yapılan işlemlerde EEG verisinin 3 saniyelik motor imgeleme kısmı üzerinde işlemler yapılmıştır. Bir sonraki adımda ise 1 saniyelik veri segmenti (0,5. ve 1,5. Saniyeden itibaren 1'er saniyelik veriler) kullanılarak sınıflandırma işlemi için korelasyon katsayısı ve kovaryans matrisleri hesaplanmıştır.

Sınıflandırmaları doğrulamak için sınıf etiketleri sıralı olarak işlenmesi yerine rastgele karıştırılarak işlenmiştir. Elde edilen sonuçlar beklendiği gibi neredeyse 0,25'e düşmüştür. Bu da sınıflandırma sonuçlarının doğruluğunu teyit etmektedir.

1 saniyelik veri segmenti için sonuçlar olumlu olduğundan, işlemler için hangi aralığın seçilmesi gerektiğini belirlemek amacıyla 3 saniyelik verinin tamamı (örnekleme hızı 250 Hz olduğu için toplam 750 örnek) analiz edilmiştir.

Seçilen 1 saniyelik segmentin sınıflandırma sonucu, 3 saniyelik sinyal üzerindeki uyaranlardan başlayarak bir örnekleme kaydırılmıştır (toplam 750 örnekleme). Her bir deneğin 500 kaydırması için sınıflandırma sonuçları hesaplanmıştır. Elde edilen verilerden ortalama, minimum ve maksimum değerler hesaplanmıştır.

İBYSA ve LDAS uygulanarak yapılan sınıflandırmalarda homojen sonuçlar elde edildiği görülmüştür. Başarı hesaplaması homojen olduğu için seçimin rastgele yapılabileceğine karar verilmiştir.

Yapılmış olan yorum ve değerlendirmeler, bir önceki adımda hesaplanan ortalamalar dikkate alınarak yapılmıştır.

Korelasyon katsayısı matrisi hesaplanan veriler için sınıflandırma sonuçları, hem Alfa hem de Beta bantları için İBYSA'nın ve hem Alfa hem de Beta bantları için LDAS'nin daha yüksek ve daha homojen değerlere sahip olduğunu göstermiştir.

Kovaryans matrisinden çıkarılan özelliklerin sınıflandırma sonuçları, hem Alfa hem de Beta bantları için İBYSA, NBS ve LDAS'nin neredeyse %100'e sahip olduğunu, ancak NBS sınıflandırmasında sınıflandırma ortalamasını etkilemeyen birkaç düşüş olduğunu göstermiştir. Kovaryans matrisi hesaplanan verilerin korelasyon katsayısı matrisi hesaplanan verilere kıyasla daha başarılı sınıflandırma sonuçlarına sahip olduğu açıkça görülebilmektedir. Kovaryans matrisi hesaplanan verilerin İBYSA, NBS ve LDAS sınıflandırma sonuçlarının başarısı ve homojenliği nedeniyle, verilerin herhangi bir "1 saniyelik segmenti" sınıflandırma için rastgele kullanılabilir. Ancak aynı durum korelasyon katsayısının, sadece İBYSA ve LDAS sınıflandırmaları için söz konusudur. NBS sınıflandırmasının başarısı ve homojenliği, korelasyon katsayısı matrisinden çıkarılan özellikler için diğer sınıflandırma yöntemleri kadar iyi olmadığı tespit edilmiştir.

Bu çalışma, özellik çıkarma yöntemi olarak hem Kovaryans hem de Korelasyon Katsayısı matrislerini kullananıldığı tek çalışmadır. BCI Competition IV Veri Seti 2a üzerinde yapılan çalışmaların sonuçları çeşitli doğruluk oranları göstermektedir. Ancak en yüksek olanı %96,9 doğruluk oranına sahip olan Ting Li ve arkadaşlarıdır (Li.T. et al,2023). Yapmış olduğumuz bu çalışma ile işlenen veri setinin başarı oranını bir adım daha ileriye taşınmıştır ki bu da kovaryans matris özellik çıkarımı ile %100 doğruluktur. Tablo 17’de BCI Competition IV 2a veri seti üzerinde yapılan bazı çalışmaların sınıflandırma sonuçları ve çalışmamızın sonuçları paylaşılmıştır.

ACKNOWLEDGEMENTS

I would like to express my gratitude to my supervisor, Assoc. Prof. Dr. Ahmet AYDIN and my former supervisor, the late Prof. Dr. Sami ARICA and , for their invaluable support throughout the process of conducting and completing this study. I am also deeply grateful to my beloved wife, Kübra, and my dear son, Hazni, for their unwavering support and understanding, despite the fact that I was not always able to spend as much time with them as I would have liked during the intensive research period. I am also indebted to my mother, Zeynep, and my late father, Hazni, for their constant encouragement and support, as well as to everyone who provided me with any kind of assistance, big or small, during my academic pursuits.

LIST OF TABLES

LIST OF FIGURES

SYMBOLS AND ABBREVIATIONS

AR-CSP	:	Artifact-rejected common spatial pattern
BBA	:	Beyin-bilgisayar arayüzü
BCI	:	Brain-computer interface
CNN	:	Convolutional Neural Network
CSP	:	Common spatial pattern
DCT	:	Discrete Cosine Trasnform
EEG	:	Electroencephalography
EEG-ARNN	:	EEG channel active inference neural network
FBCSP	:	Filter Bank Common Spatial Pattern
FBRTS	:	Filter Banks and Riemannian Tangent Space
FBTSCORAL	:	Correlation Alignment in Filter Bank Riemannian Tangent Space
FFNN	:	Feed Forward Neural Network
İBYSA	:	İleri Beslemeli Yapay Sinir Ağı
LDAC	:	Linear Discriminant Analysis Classifier
LDAS	:	Lineer Diskriminant Analizi Sınıflandırıcı
MI	:	Motor imagery
NBC	:	Naive Bayes Classifier
NBS	:	Naive Bayes Sınıflandırıcı
NCFS	:	Neighborhood component feature selection
OSTFR	:	Optimized spatio-temporal feature representation
RICA	:	Reconstruction Independent Component Analysis
RCSP	:	Regularized Common Spatial Pattern
OSTFR	:	Optimized spatio-temporal feature representation
SRSG-FasArt	:	Self-regulated supervised Gaussian fuzzy adaptive system Art
SR-FBCSP	:	Shrinkage Regularized Filter Bank Common Spatial Pattern
SVM	:	Support Vector Machines

1. INTRODUCTION

1.1. Brain-Computer Interface

A brain-computer interface (BCI) is a technology that enables a direct communication pathway between the electrical activity of the brain and an external device, such as a computer or a prosthetic limb. This technology has the potential to revolutionize the way we interact with machines. For instance, BCIs can help individuals who are paralyzed to control computers or prosthetic limbs with their thoughts. Additionally, they can aid in the detection and diagnosis of various disorders, including epilepsy.

There are three types of BCIs: noninvasive, invasive, and partially invasive. Invasive BCIs require surgery to implant electrodes directly into the brain, which can provide the highest quality signal but also carry the greatest risk of infection and other complications. Noninvasive BCIs use electrodes placed on the scalp to measure brain activity and are safer than invasive BCIs but can be less accurate. Partially invasive BCIs are implanted inside the skull, with the rest of the device outside the brain, resulting in better signal resolution than noninvasive BCIs.

Overall, a brain-computer interface (BCI) is a means of communication between the human brain and machines, such as computers, using electroencephalography (EEG) signals. With further research and development, BCIs have the potential to greatly improve the lives of individuals with disabilities and other medical conditions. (Rabie R. et al 2015), (Sharma V., Aug 2020).

1.2. Electroencephalogram (EEG)

The study of EEG signals dates back to the early 20th century. In 1929, Hans Berger provided an interpretation of the electrical activity of brain tissue neurons, which marked the beginning of EEG research and modern neural science. Through numerous experiments, Berger proved his hypothesis and determined the frequency band of the brain wave of the human cerebral cortex, ultimately proving the existence of Alpha rhythm. Since then, humans have gained a preliminary understanding of the common electrical activity rules of the human brain. However, until the 21st century, our knowledge of EEG signals was limited, and the complex structure of the brain remained an important, mysterious subject for scientists (Berger H., 1929)

The Electroencephalogram (EEG) is a valuable and unique method of measuring the electrical properties of the brain. It is the most used noninvasive technique for recording brain activity and is widely used in many noninvasive BCI systems due to its simplicity and low cost. (Greenfield L. et al, 2012).

Figure 1 shows noninvasive EEG electrode placement which is one of the most commonly used methods.

Figure 1. Noninvasive EEG bonnet placed head

EEG Generation:

An EEG signal measures the electrical currents that flow through the dendrites of many pyramidal neurons in the cerebral cortex when they are stimulated (Figure 2). These currents create a magnetic field which can be measured by Electromyogram (EMG) equipment. The EEG system, on the other hand, measures the secondary electrical field generated across the scalp.

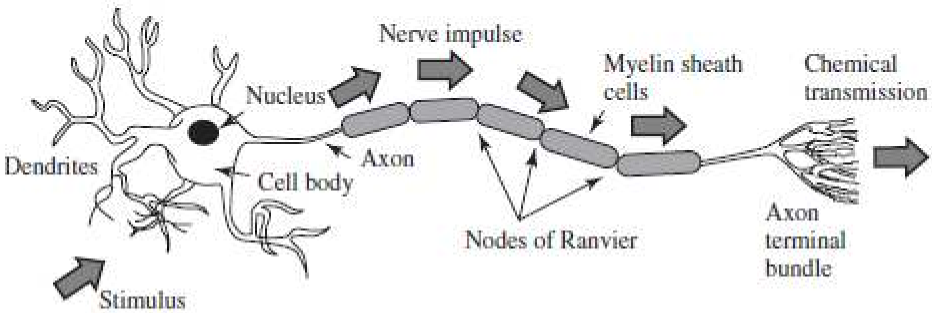

Figure 2. Stimulus on the structure of a neuron

Differences in electrical potentials in the brain are created by the combined effects of graded potentials from pyramidal cells. These graded potentials cause electrical dipoles between the soma (the body of a neuron) and apical dendrites that branch from neurons. The brain's current is primarily generated by pumping positive ions, such as sodium (Na^+), potassium (K^+), calcium (Ca^{++}), and negative ions like chlorine (Cl^-), through the neuron membranes in the direction determined by the membrane potential (Chambers J.A. and Sanei S.,2007).

EEG Rhythms:

When a neuron is stimulated, its membrane potential changes, which can trigger an action potential. This is a brief surge of electrical activity that travels down the neuron's axon. In the brain, groups of neurons often fire together in synchrony, generating electrical currents that EEG electrodes can detect. The EEG signal reflects the summed electrical activity of these synchronized neuronal populations and is a complex waveform with various frequencies and amplitudes. The different frequencies in the signal are associated with different brain states.

The EEG signal is not a random collection of electrical activity. Instead, it exhibits rhythmic activity at different frequencies, which are classified into different bands based on their frequency range. Delta waves (0.1-4 Hz) are associated with deep sleep, while theta waves (4-8 Hz) are linked to drowsiness, early stage of sleep, and daydreaming. Alpha waves (8-12 Hz) are associated with a relaxed but alert mind, and they are prominent when a person is closing their eyes or resting quietly. Beta waves (13-30 Hz) are linked to active wakefulness, focused attention, and problem-solving. Finally, gamma waves (30-100 Hz) are high-frequency waves and are associated with higher-order cognitive functions such as perception, learning, and memory (Nayak S.C., Anilkumar C.A., 24 Jul 2023).

The electrical currents produced by the brain are not very strong when they reach the surface of the scalp. The skull and scalp act as conductors, which causes the spatial resolution of the EEG signal to be blurred. This means that the activity recorded by a particular electrode reflects the behavior of a large area of the brain beneath it, not solely the activity of neurons that are located directly below the electrode. Nevertheless, despite this limitation, EEG provides valuable information about the overall electrical activity of the brain. (Li, X. et al, 2021).

1.3. Motor imagery:

Motor imagery is the practice of mentally performing a motor act without any physical movement (Figure 3). It is generally agreed that similar brain regions and functions are utilized when imagining a motion in the mind. (Neuper C. and Pfurtscheller G, 1996)

Figure 3. Motor imagery

Figure 4 shows the human brain motor region.

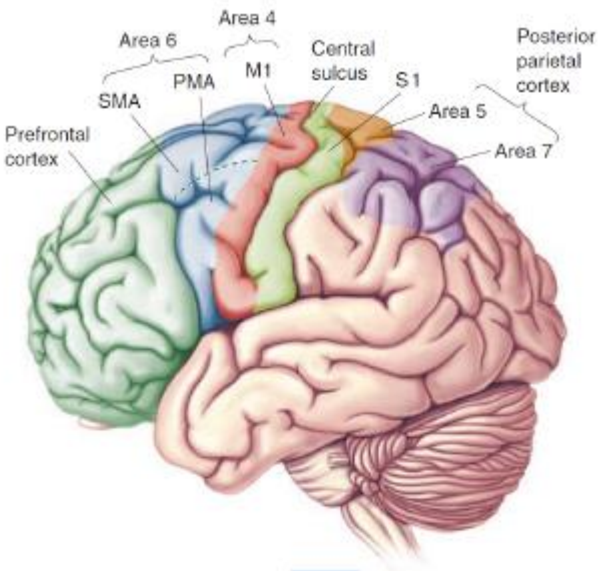

Figure 4. Human brain motor region M1 (Tortora, G.J.; Derrickson, B, 2011)

Motor imagery (MI) is a powerful technique that can revolutionize the brain-computer interface (BCI) applications, including the gaming industry. By imagining body movements instead of actual movement, MI can enhance the user's immersive experience and take it to a whole new level (Djamal C. et al, 2017).

1.4. Signal Preprocessing:

1.4.1. Filtering - Common Average Referencing (CAR):

The common average reference (CAR) technique is used in EEG signal processing to subtract the value of a specific channel of interest from the average value of the entire electrode montage. This results in a spatial voltage distribution with a mean of zero, assuming that the entire head is covered with equally spaced electrodes and the potential on the skull is produced by point sources. (Bertrand et al. ,1985).

Although it is rare to achieve uniform and total electrode coverage and point sources in practice, the Common Average Reference (CAR) method offers practically reference-free EEG recording. The CAR method eliminates components in a significant fraction of the electrode population, highlighting components with highly focused distributions. This makes it act as a high-pass spatial filter (Nunez et al., 1985). However, minor or nonexistent elements in the electrode of interest, but present in most of the electrode population, may appear in CAR recordings as "ghost potentials." (Desmedt et al. ,1990).

1.4.2. Analysis – Periodogram:

The periodogram is a widely used tool in frequency domain analysis to detect unknown deterministic signals. It calculates the power spectral density (PSD) or mean-square spectrum (MSS) of the input time samples by averaging the squared magnitude of the finite Fourier transform (FFT) computed over windowed input of a certain size. This tool is fundamental in signal processing as it analyzes the frequency content of a signal and displays the distribution of its power across different frequencies. It is particularly useful in examining the power distribution of EEG signals. (Olabiyi O., Annamalai A., 2012)

The periodogram is a fundamental method for estimating the power spectrum of a random process. It has clear physical meaning, a simple calculation process, and high efficiency. Spectral estimation is an important branch of digital signal processing that is used to investigate the features of signals in the frequency domain. The aim of spectral estimation is to extract useful information about signals in the frequency domain from noisy infinite time series by ascertaining their power spectrum based on a series of limited observed data. (Zhiqiang S. et al, 2012).

1.5. Feature Extraction in EEG signal processing

Biomedical signal analysis involves a crucial stage called feature extraction, which comes after signal preprocessing. In the medical field, acquiring data across several hours and channels, as in the case of EEG signal acquisition, is necessary, which has led to the growing popularity of working with big data. Data compaction and dimensionality reduction are the two main objectives of feature extraction. By using a smaller subset of features, one can effectively represent their data, which enables the implementation of artificial intelligence (AI) and machine learning (ML) algorithms for applications such as diagnosis and categorization. (Subasi, A. ,2019).

The used feature extraction methods used in this study are listed below:

1.5.1. Reconstruction Independent Component Analysis:

Reconstruction Independent Component Analysis (RICA) is an unsupervised algorithm for feature learning that is an extension of Independent Component Analysis (ICA). RICA is designed to extract the most relevant features from data in an easy and accurate way (Lei Y. et al, 2016).

The mathematical definition for rICA is a follows:

$$X = A \,.\, S \qquad (1.5.1.1)$$

Where X is the matrix for EEG signals (channels x time samples), A is the mixing matrix representing the contribution of each independent source to each channel, S is the matrix of independent components, which are the sources we aim to extract.

After the S obtained by implementing ICA, S being analyzed based on relevency to neural activity. Relevent components of S, which is $S_{relevent}$,are being retained and rest of the component which correspnds to noise or artifact are being suppressed.

Then a clean signal is being reconstructed with modified components:

$$X_{reconstructed} = A \,.\, S_{relevent}$$ (Lei Y. et al, 2016). (1.5.1.2)

1.5.2. Discrete Cosine Transform:

The discrete cosine transform is a versatile tool that can be used in a variety of applications, including frequency spectrum analysis, data compression, convolution computation, and information hiding. With its ability to efficiently process large amounts of data, this transform is an essential tool for anyone who needs to analyze and manipulate digital information with precision and accuracy. By using the discrete cosine transform, you can gain new insights into your data and unlock new possibilities for innovation and discovery. (Zhou J., Chen P., 2009).

The Discrete Cosine Transform (DCT) is a commonly used method for converting time series signals into basic frequency components. It is particularly useful for data compression as it allows for a reduction in data size without losing important information. One key advantage of the DCT is that it concentrates the energy of correlated input data on the first few transform coefficients, making it an effective feature extraction technique. This means that the other coefficients can be safely ignored without significant loss of information. (Birvinskas D. et al, 2012)

The mathematical definition of Two-Dimensional Discrete Cosine Transform:

Let x[m,n] be a two dimensional signal or matrix of size M x N. The two dimensional descrete cosine transform defined as,

$$x[k,l] = \alpha(k)\alpha(l)\sum_{m=0}^{M-1}\sum_{n=0}^{N-1} x\,[m,n]\cos\left[\frac{\pi}{M}\left(m+\frac{1}{2}\right)k\right]\cos\left[\frac{\pi}{N}\left(n+\frac{1}{2}\right)l\right] \qquad (1.5.2.1)$$

for k = 0,1,2,…,M-1 and l = 0,1,2,…,N-1

normalization factor $\alpha(p)$:

$$\alpha(p) = \begin{cases} \sqrt{\frac{1}{M}} & if\ \ p = 0 \\ \sqrt{\frac{2}{M}} & if\ \ p > 0 \end{cases} \qquad (1.5.2.2)$$

Where $p = k\ or\ l$ (Gonzalez and Woods, 2008).

1.5.3. Coherence:

Understanding the human brain is essential to unravel the mysteries of neuroscience and unlock the secrets of large-scale brain networks. The microstructure of the cerebral cortex shows long-range connectivity, which is a crucial aspect of neuroscience. By using brain activity coherence, we can recognize and understand this complex connectivity. This is crucial because each neuron's activity is a closed problem, but when they communicate, the group activity becomes intricate, forming an extensive network. By understanding these relationships, we can gain a deeper insight into the inner workings of the brain and further improve our knowledge of neuroscience. (Schneider M. et al, 2021).

Cross-spectral or frequency coherence is a method to evaluate the coherence between two signals that have similar statistical properties. On the other hand, partial coherence is used to compare two different versions of the same signal, either during the process of interest or after removing confounding variables. When examining the relationship between different epochs of the same signal (i.e., between a channel and itself), it is referred to as "near coherence" or magnitude square coherence. (Fallani F.D.C et al, 2021).

The mathematical definition of coherence:

Given two EEG signals $x(t)$ and $y(t)$, the coherence $C_{xy}(f)$ at frequency f defined as,

$$C_{xy}(f) = \frac{|p_{xy}(f)|^2}{R_x(f) \cdot P_{yy}(f)} \tag{1.5.3.1}$$

Where,

$p_{xy}(f)$is the cross spectral density of signal $x(t)$ and $y(t)$,

$p_{xy}(f) = E[X(f) \cdot Y^* (f)]$

Where $X(f)$ and $Y(f)$ are the fourier transform of the signal $x(t)$ and $y(t)$, and $*$denotes the complex conjugate.

$p_{xx}(f)$ and $p_{yy}(f)$ are the power spectral density of signal $x(t)$ and $y(t)$,

$p_{xx}(f) = E[|X(f)|^2]$, $p_{yy}(f) = E[|Y(f)|^2]$

$|\cdot|$ donates the magnitude, and $E[\cdot]$ represent the expected value (Nunezand Srinivasan, 2006).

1.5.4. Correlation Coefficient Matrix:

The correlation coefficient is a statistical measure that helps to determine the strength and direction of a linear relationship between two variables. It ranges from -1 to 1, where 1 represents a perfect positive correlation, meaning that as one variable increases, the other also increases in proportion. On the other hand, -1 signifies a perfect negative correlation, which indicates that if one variable increases, the other will decrease proportionally. A value of 0 indicates no linear correlation between the variables.

In the field of EEG signal processing, the correlation coefficient is a useful tool for analyzing the relationships between different channels of recorded brain activity. Correlation coefficients can be extracted from EEG data and used to identify features that may be helpful in classification tasks

The correlation coefficient of two random variables is a measure of their linear dependence. If each variable has N scalar observations, then the Pearson correlation coefficient is defined as

$$\rho(A, B) = \frac{1}{N-1} \sum_{i=1}^{N} \left(\frac{A_i - \mu A}{\sigma A}\right) \left(\frac{B_i - \mu B}{\sigma B}\right) \tag{1.5.4.1}$$

where μA and σA are the mean and standard deviation of A, respectively, and μB and σB are the mean and standard deviation of B. Alternatively, you can define the correlation coefficient in terms of the covariance of A and B:

$$\rho(A,B) = \frac{\mathrm{cov}(A,B)}{\sigma A \sigma B} \tag{1.5.4.2}$$

The correlation coefficient matrix of two random variables is the matrix of correlation coefficients for each pairwise variable combination,

$$R = \begin{pmatrix} \rho(A,A) & \rho(A,B) \\ \rho(B,A) & \rho(B,B) \end{pmatrix} \tag{1.5.4.3}$$

Since A and B are always directly correlated to themselves, the diagonal entries are just 1, that is,

$$R = \begin{pmatrix} 1 & \rho(A,B) \\ \rho(B,A) & 1 \end{pmatrix} \tag{1.5.4.4}$$

(Kendall M.G, 1979)

1.5.5. Covariance Matrix:

A covariance matrix is a square matrix that captures the covariances between all pairs of features (variables) in a given dataset. In simpler terms, covariance indicates how two features vary together. It represents the tendency of two features to move together. A positive covariance suggests that they increase or decrease together, while a negative covariance indicates that they move in opposite directions. A value close to zero implies little to no linear relationship between the two features.

Electroencephalogram (EEG) signals are complex and often noisy, which makes covariance matrices valuable for understanding the relationships between different brain regions. In EEG data, the multiple electrodes (channels) can be treated as features. The covariance matrix summarizes the covariances between these channels, revealing how different brain areas interact.

For two random variable vectors A and B, the covariance is defined as

$$\mathrm{cov}(A,B) = \frac{1}{N-1} \sum_{i=1}^{N} (A_i - \mu A) * (B_i - \mu B) \tag{1.5.5.1}$$

where μA is the mean of A, μB is the mean of B, and * denotes the complex conjugate.

The covariance matrix of two random variables is the matrix of pairwise covariance calculations between each variable,

$$C = \begin{pmatrix} \text{cov}(A, A) & \text{cov}(A, B) \\ \text{cov}(B, A) & \text{cov}(B, B) \end{pmatrix} \quad (1.5.5.2)$$

For a matrix A whose columns are each a random variable made up of observations, the covariance matrix is the pairwise covariance calculation between each column combination. In other words,

$$C(i, j) = \text{cov}(A(:, i), A(:, j)) \quad (1.5.5.3)$$

(Mathworks 1,2024)

In statistical analysis, the matrix of correlation coefficients is the preferred choice when a standardized measure of the linear relationship between variables is needed, regardless of the scale on which they are measured. This is especially relevant in the EEG analysis, where the focus is on determining the strength of the relationships between different brain regions, rather than specific voltage values. On the other hand, the covariance matrix is crucial when you want to understand the raw covariation between variables and their direction of change. It is particularly useful when analyzing data in their original units, as it provides a more meaningful understanding of the data.

1.6. Classification methods:

1.6.1. Feed Forward Neural Network:

A feedforward neural network, also known as a feedforwardnet, is a fundamental architecture in artificial intelligence, especially in deep learning. It is characterized by a unidirectional flow of information that processes data from an input layer through hidden layers to an output layer. A feedforwardnet is made up of multiple layers of interconnected artificial neurons called perceptrons. The Input Layer receives the initial data, while the hidden layers carry out the primary computations and information extraction. There can be one or more hidden layers in the network. The output Layer is the most critical component in a feedforward neural network because it produces the final result or prediction. Every neuron in a layer connects to all neurons in the subsequent layer, and these connections hold weights that determine the influence of one neuron on another. Feedforward networks learn by adjusting the weights of connections between neurons, which is usually accomplished using backpropagation, a training algorithm. This algorithm compares the network's output with the desired output and adjusts weights iteratively to minimize the error (Mathworks 2,2024).

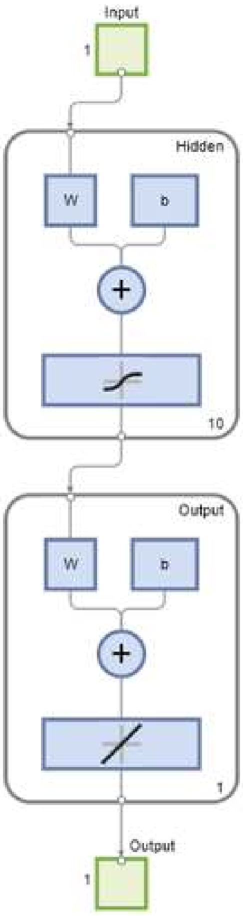

Figure 5. An example of feedforwardnet block diagnram (Mathworks 2,2024)

1.6.2. Naive Bayes Classifier:

The Naive Bayes (NB) classifier algorithm uses Bayesian probability to predict the class of a given data. The core of Naive Bayes is a simple mathematical theorem, the Bayes's Theorem. Compared to other algorithms, this algorithm requires a smaller training set to build a model. It is also modest in dealing with the size of the training set. This classification technique has no trouble handling missing values, as the computation is based solely on variable conditional probability. Using this algorithm does not require data normalization (pre-processing). It can quickly predict some types of problems and is particularly useful for working with many classes in the data (Chen, H.,2021).

Naive Bayes classification (fitcnb) function of MatLab (Mathworks) used for NB classification. The fitcnb function estimates the conditional probability distribution of each feature for each class. It assumes independence between features, so the joint probability is the product of individual feature probabilities.

Prediction process:

Given a new data point $X_{new} = [x_1, x_2, \ldots, x_d]$, the classifier predicts the class C_k that maximizes the posterior probability,

$$P(C_k|X_{new}) \; \alpha \; P(C_k) \; \prod_{i=1}^{d} P(x_i|C_k) \tag{1.6.2.1}$$

Where, $P(C_k)$is Prior probability of class C_k, $P(x_i|C_k)$ is conditional probability of feature x_i given class C_k (Hastie et al, 2008).

1.6.3. Linear Discriminant Analysis Classifier:

Linear Discriminant Analysis (LDA) is a powerful machine learning technique used for classification problems. It is a supervised learning method that is great at classifying data points into predefined categories. LDA learns from labeled data, which is data that already has known class membership, and then uses this knowledge to classify new and unseen data points. LDA assumes that the data for each class follows a Gaussian distribution, which is a multivariate distribution consisting of multivariate Gaussian distribution components. Each component is defined by its mean and covariance. The mixture is further defined by a vector of mixing proportions, where each mixing proportion represents the fraction of the population described by a corresponding component. LDA analyzes these distributions to find a linear hyperplane that best separates the classes.

Fit discriminant analysis classifier (fitcdiscr) function of MatLab (Mathworks) used for LDA classification. fitcdiscr estimates the mean and covariance for each classes. It computes discriminant function for each class based on the training data. LDA assumes all classes share same the same covariance matrix.

Discriminant function:

$$g_k(x) = \log\big(P(C_k)\big) - \frac{1}{2}\log(|\Sigma_k|) - \frac{1}{2}(x - \mu_k)^T \Sigma_k^{-1}(x - \mu_k) \tag{1.6.3.1}$$

Where, $P(C_k)$prior probablity of class k, μ_k is mean vector of class k, Σ_k is covariance matrix of class k, x is input data point.

For a given input x, the classifier evaluates $g_k(x)$ for each class k and assigns x to the class with the highest discriminant function value to perform prediction (Mathworks 3,2024).

2. LITERATURE REVIEW

There are a variety of implementations of MI classifications with different methods of analysis. Some examples of these methods are the Pearson correlation coefficient, the correlation of EGG signals in sculp regions, averaging covariance, principal component analysis, and independent component analysis (Li K. et al 2009, Li C. et al May 2022, Hung CI. Et al2005, Pawan et al 2023).

However, if we focus on the BCI Competition IV 2a data set, which has been used in various studies:

Feifei Qi et al. (Qi F. et al ,2021), on the same data set, the results from Correlation Alignment in Filter Bank Riemannian Tangent Space (FBTSCORAL) proposed method report the ablation study with an accuracy of %76.77.

Badamchizadeh et al. (Badamchizadeh M.A. et al,2018), on the same data set An artifact-rejected common spatial pattern (AR-CSP) method was proposed for feature extraction using LDA as a classifier, with a success rate of %81.33. And common spatial pattern (CSP) method was proposed for feature extraction “self-regulated supervised Gaussian fuzzy adaptive system Art (SRSG-FasArt)” as a classifier, with a success rate of %85.49.

Florian Yger (Yger F., 2013), on the same data set, Common Spatial Pattern (CSP) was proposed for feature extraction and Support Vector Machines (SVM) as a classifier, with a success rate of %79.17 on normalized data.

Puthusserypady et al.(Puthusserypady et al), on the same data set, Filter Bank Common Spatial Pattern (FBCSP), Convolutional Neural Network (CNN)-based algorithms with an accuracy of %68.5.

Szu-Chi Huang et al. (Huang S-C. et al, 2023), on the same data set, proposed CSP and Riemannian tangent space as features and SVM distance analysis for classification with an accuracy of %76.82.

Hua Fang et al. (Fang H. et al,2022), on the same data set, propose a fusion method combining Filter Banks and Riemannian Tangent Space (FBRTS) with a classification accuracy of %77.7.

Lijun Yang et al.(Yang L. et al,2022), on the same data set, proposed Regularized Common Spatial Pattern (RCSP) as feature extraction and Binary Classification Model with an accuracy of %87.04.

Dharmendra Gurve et al. (Gurve D. et al,2019), on the same dataset, proposed Riemannian geometry in the manifold of covariance matrices, and neighborhood component feature selection (NCFS) algorithm as feature extraction, and a convolutional neural network (CNN) for classification with a %77.91 classification accuracy.

Qinkun Xiao et al. (Xiao Q. et al,2023), on the same data set, propose a 3D-CNN MI decoding method with optimized spatio-temporal feature representation (OSTFR), leading to decoding accuracies of %87.24.

H. Vikram Shenoy et al. (Shenoy H.V. et al,2015), on the same data set, proposed Shrinkage Regularized Filter Bank Common Spatial Pattern (SR-FBCSP) feature extraction and Support Vector Machine Classifier with an accuracy of %82.0656.

Ting Li. et al. (Li.T. et al,2023), on the same data set, proposed an end-to-end deep learning framework called EEG channel active inference neural network (EEG-ARNN) with the success of classification accuracy %96.9 EEG-ARNN.

Syed Umar Amin et al. (Amin S.U. et al,2020), on the same data set, propose a feature fusion model Multi-CNN fusion method with a success rate of %74.8.

When examining other studies that have employed the methods used in our research, the number of studies utilizing correlation coefficients and covariance matrices for feature extraction is quite limited. When conducting a literature review while disregarding studies that have used the same dataset, the number of studies utilizing the methods we have used remains limited. Below are some of the studies where these methods have been applied and developed:

Y. Park and W. Chung (Y. Park and W. Chung, 2020), introduces a feature extraction method for EEG-based cognitive task classification by analyzing the correlation coefficients among EEG channels. The approach aims to enhance classification accuracy by capturing the inter-channel dependencies inherent in EEG signals. Study reaches with a success rate of %81.5 classification accuracy.

Rahman MM and Fattah SA. (Rahman MM, Fattah SA.,2017), presents a classification scheme for mental tasks using correlation coefficient features derived from intrinsic mode functions of EEG signals. The method focuses on inter-channel correlation features and intrachannel statistical features to form a comprehensive feature matrix for classification. Study reaches with a success rate of %99 classification accuracy

Carrara I., and Papadopoulo T. (Carrara I., and Papadopoulo T.,2023), proposes a framework for classifying Brain-Computer Interface (BCI) EEG signals using augmented covariance matrices derived from autoregressive models. The approach incorporates both spatial and temporal information, enhancing the classification performance for motor imagery tasks. Study reaches with a success rate of %99 classification accuracy.

Our study differs from existing studies that used the same dataset. Because the methods we employed are the fundamental techniques for feature extraction applicable in linear classification, and they are notable for their effectiveness. Furthermore, this study is the only one that used both Covariance and Correlation Coefficient matrices as feature extraction methods and FFNN, NBC, and LDAC were used as classification methods.

3. MATERIAL AND METHOD

3.1. Dataset:

The data set 2a of the BCI Competition IV (Brunner C. et al., 2008) is widely known to researchers. This data set consists of EEG data from 9 subjects. The cue-based BCI paradigm consisted of four different motor imagery tasks (would be named as class also), namely the imagination of movement of the left hand (class 1), right hand (class 2), both feet (class 3), and tongue (class 4). Two sessions on different days were recorded for each subject. Each session is comprised of 6 runs separated by short breaks. One run consists of 48 trials (12 for each of the four possible classes), yielding 288 trials per session.

22 Ag/AgCl electrodes (with inter-electrode distance of 3.5 cm) were used to record the EEG; the electrode placement is shown in Figure 6 Left. All signals were recorded as monopolar, with the left mastoid serving as reference and the right mastoid as ground. The signals were sampled with 250 Hz and bandpass filtered between 0.5 and 100 Hz. The sensitivity of the amplifier was set to 100 μV. An additional 50 Hz notch filter was enabled to suppress line noise.

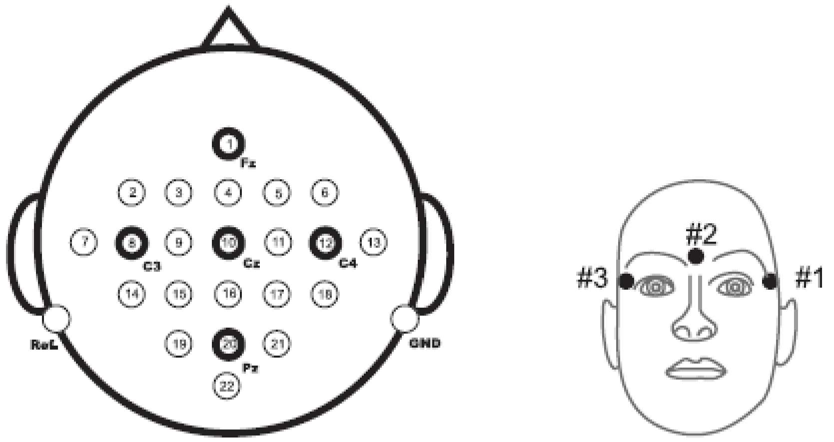

Figure 6. Left: Electrode montage corresponding to the international 10-20 system
Right: Electrode montage of the three monopolar EOG channels

In addition to the 22 EEG channels, three monopolar EOG channels were recorded (Figure 6 Right). However, in this study, only the EEG data of the 22 electrodes were used.

The time course of the experiment is summarized in Figure 7.

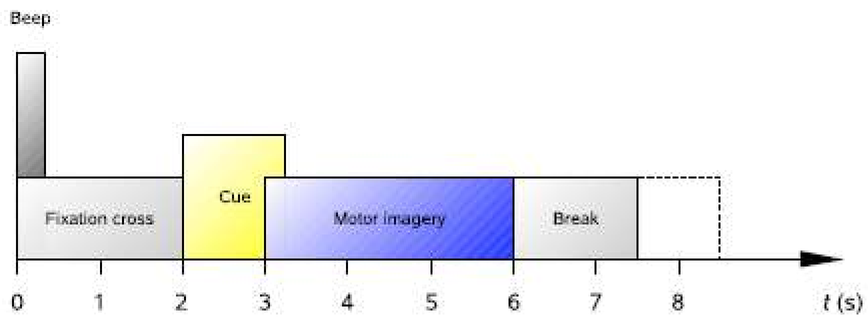

Figure 7. Timing scheme of the paradigm

All data sets were stored in the General Data Format for biomedical signals (GDF), one file per subject and session.

ID	File Name
1	A01T.gdf
2	A02T.gdf
3	A03T.gdf
4	A04T.gdf
5	A05T.gdf
6	A06T.gdf
7	A07T.gdf
8	A08T.gdf
9	A09T.gdf

Event type		Description
276	0x0114	Idling EEG (eyes open)
277	0x0115	Idling EEG (eyes closed)
768	0x0300	Start of a trial
769	0x0301	Cue onset left (class 1)
770	0x0302	Cue onset right (class 2)
771	0x0303	Cue onset foot (class 3)
772	0x0304	Cue onset tongue (class 4)
783	0x030F	Cue unknown
1023	0x03FF	Rejected trial
1072	0x0430	Eye movements
32766	0x7FFE	Start of a new run

Figure 8. Left: List of files contained in the data set
Right: List of event types (with decimal and hexadecimal values)

3.2. Methods:

3.2.1. EEG Data, pre-processes of EEG signal:

The MI signal portion of the data set corresponding to the signal from 3 to 6 seconds was used in this study (Figure 9). 22 EEG channel data were used, and 3 EOG channel data were excluded.

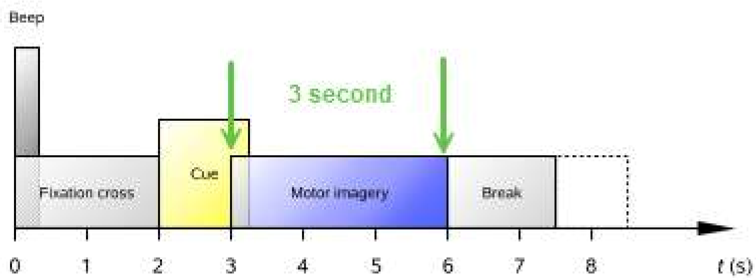

Figure 9. The Motion Imagery (MI) portion of the timing scheme

Considering the layout of the electrodes and the electrode system, the electrodes were named as follows to be used in the brain mapping:
Channel_list={'Fz','FC3','FC1','FCz','FC2','FC4','C5','C3','C1','Cz','C2','C4','C6','CP3','CP1','CPz','CP2','CP4','P1','Pz','P2','POz'};

Signal processing was done in the Matlab (Mathworks Inc.) environment. This study used the MI signal portion of the data set corresponding to the signal from 3 to 6 seconds. Before processing any data, the missing samples of the raw EEG data were filled with zeros. The data set was separated into categories according to the event type label explained in the data set description file. Figure 8 Right shows a list of event types.

One of the subjects and one of the classes were selected randomly (A1T—Class 1), and the signal for 22 channels was visualized. Figure 10 shows Subject 1- EEG Signals of the 22 channels for 3 seconds.

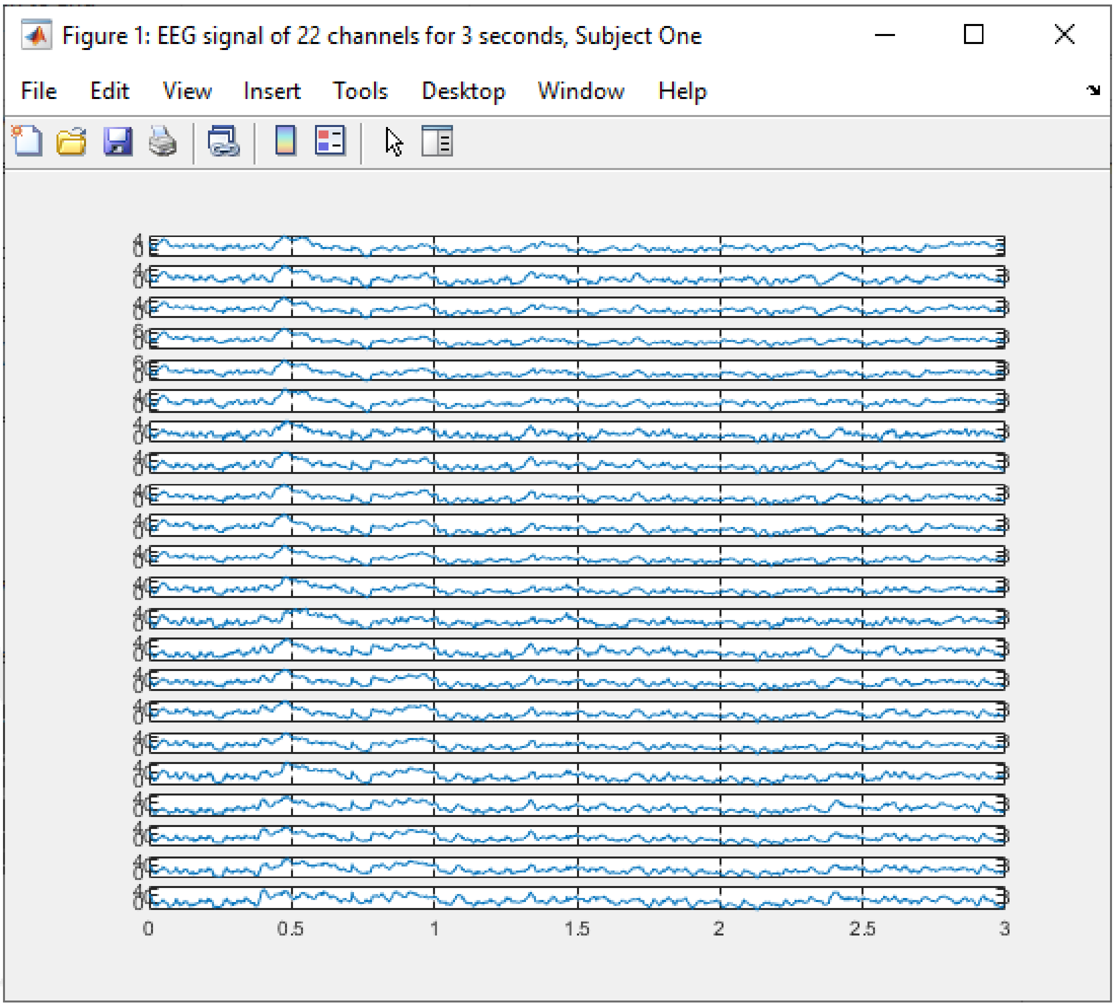

Figure 3. Subject 1- EEG Signals of the 22 channels for 3 seconds

3.2.2. Electrode Topology:

In electroencephalography (EEG), electrode topology refers to the specific arrangement of electrodes on the scalp. These electrodes record the electrical activity of the brain. The electrodes in this dataset were positioned according to a standardized 10-20 system as described in the dataset description document.

At this stage of the study, the power of the signal and mean of the third dimension, which is 72 trials, were calculated. Subject 1's brain topology was visualized according to these calculations to see electrical activity on electrodes. Figure 11 shows Subject 1's EEG electrode topology and electrical activity.

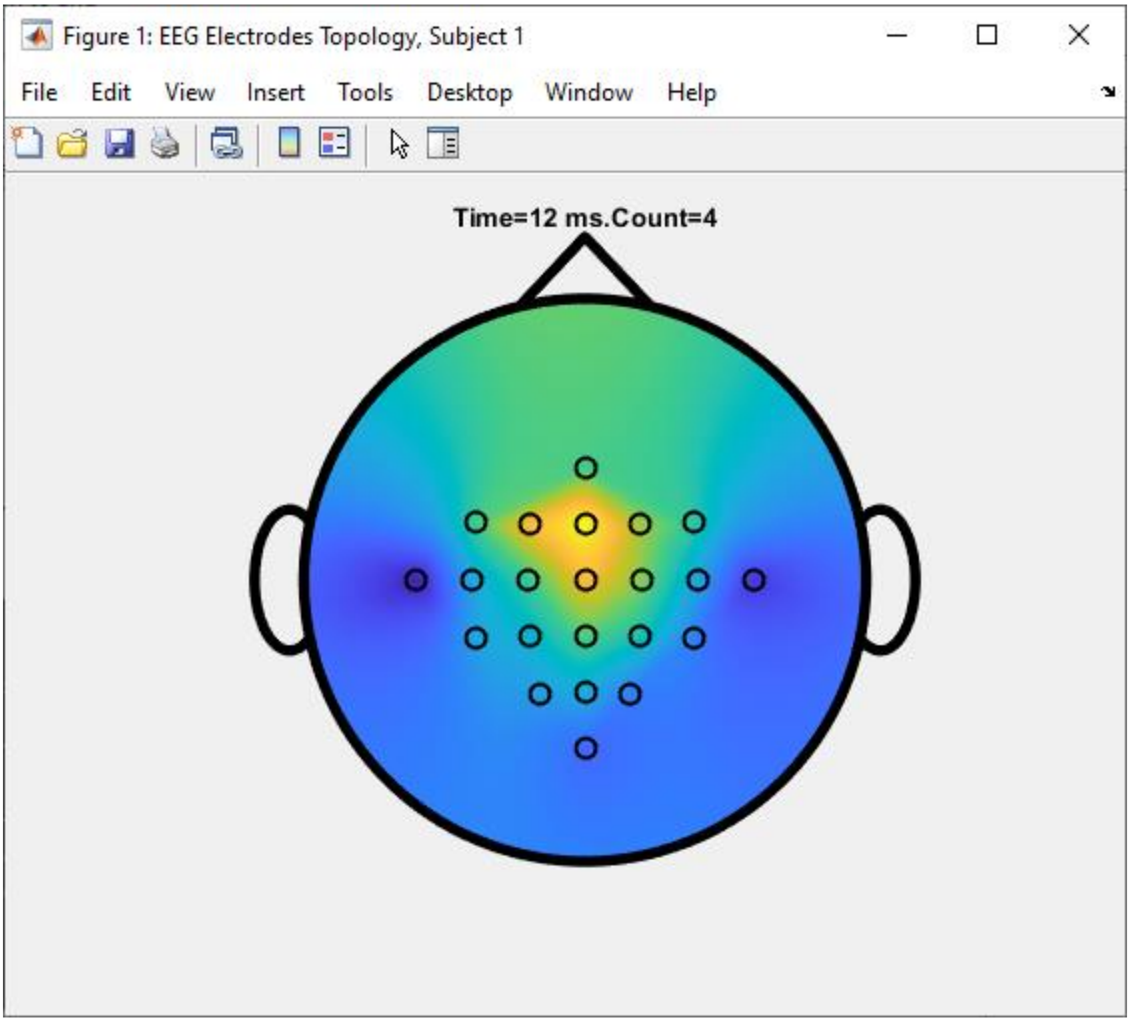

Figure 4. Subject 1- EEG electrodes topology

3.2.3. Common Averaging:

The common averaging method for EEG signals is commonly referred to as Common Average Referencing (CAR). It is a technique used to remove background noise from EEG data. The average electrical activity across all electrodes is calculated. This average is then subtracted from the recording of each individual electrode.

By subtracting the common average, background noise that affects all electrodes similarly is reduced. This can improve the signal-to-noise ratio, making the specific activity of the brain clearer.

For this stage of the study, Signals for Subject 1 were normalized using the Common Averaging method. Brain mapping was done according to the electrical activity of the electrodes. Figure 12 shows Subject 1's EEG brain mapping after common averaging.

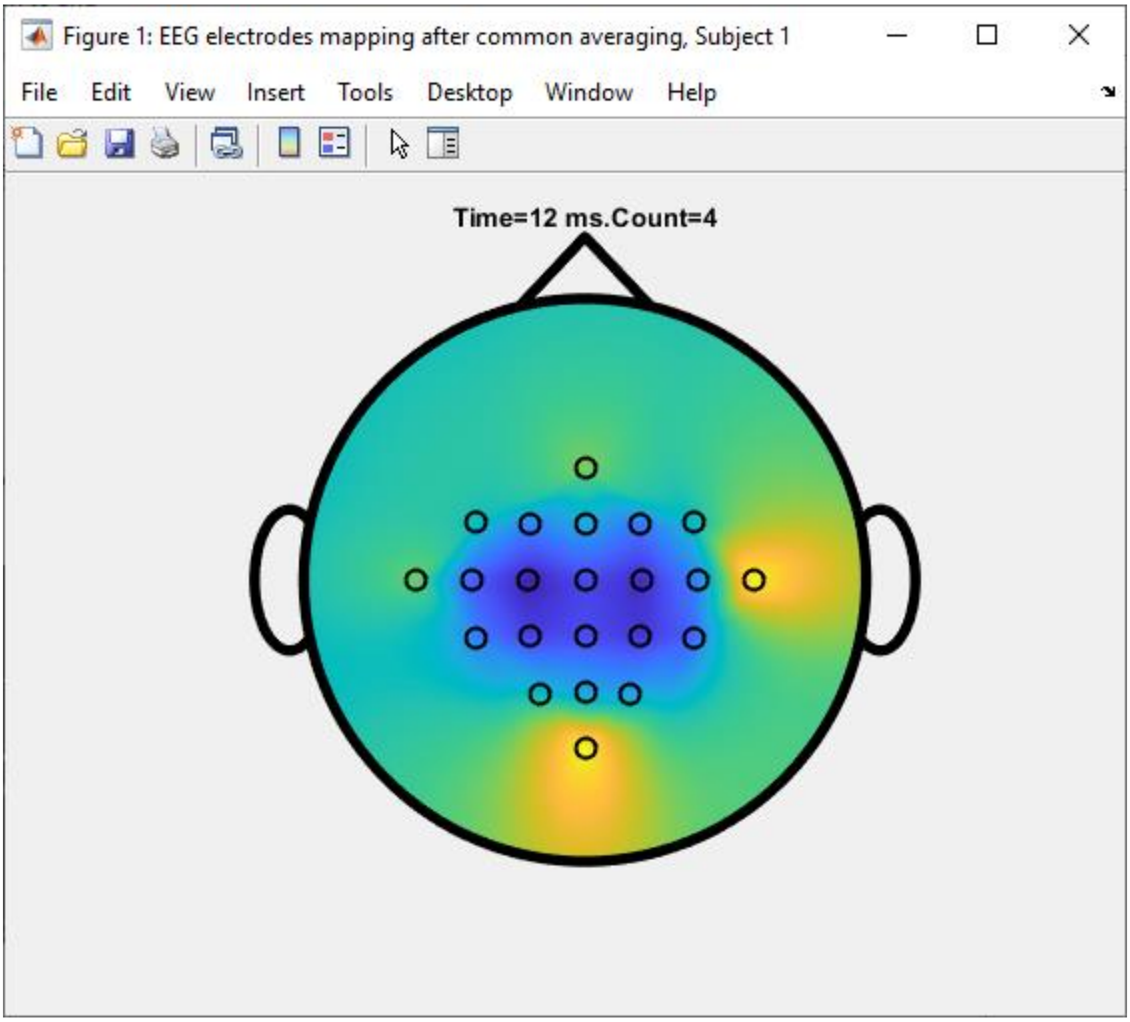

Figure 5. Subject 1- EEG brain mapping after common averaging

3.2.4. Periodogram Calculation:

A periodogram is a basic estimate of a signal's power at different frequencies. It shows the distribution of frequencies within a signal.

The primary objective of a periodogram is to estimate the power spectral density (PSD) of a signal. The PSD, a key metric in signal analysis, reveals how the power of the signal is distributed across different frequencies, providing valuable insights into the signal's behavior.

In this step, a periodogram is used as a quick and easy way to get a general idea of the frequencies present in subjects' EEG signals. Signals changed from the time domain to the frequency domain via periodogram calculation for every subject individually. Moreover, it is visualized as a graphic demonstration. Figure 13 shows periodogram graphs for all subjects for all frequency spectrums of this study, which is 0 Hz-125 Hz.

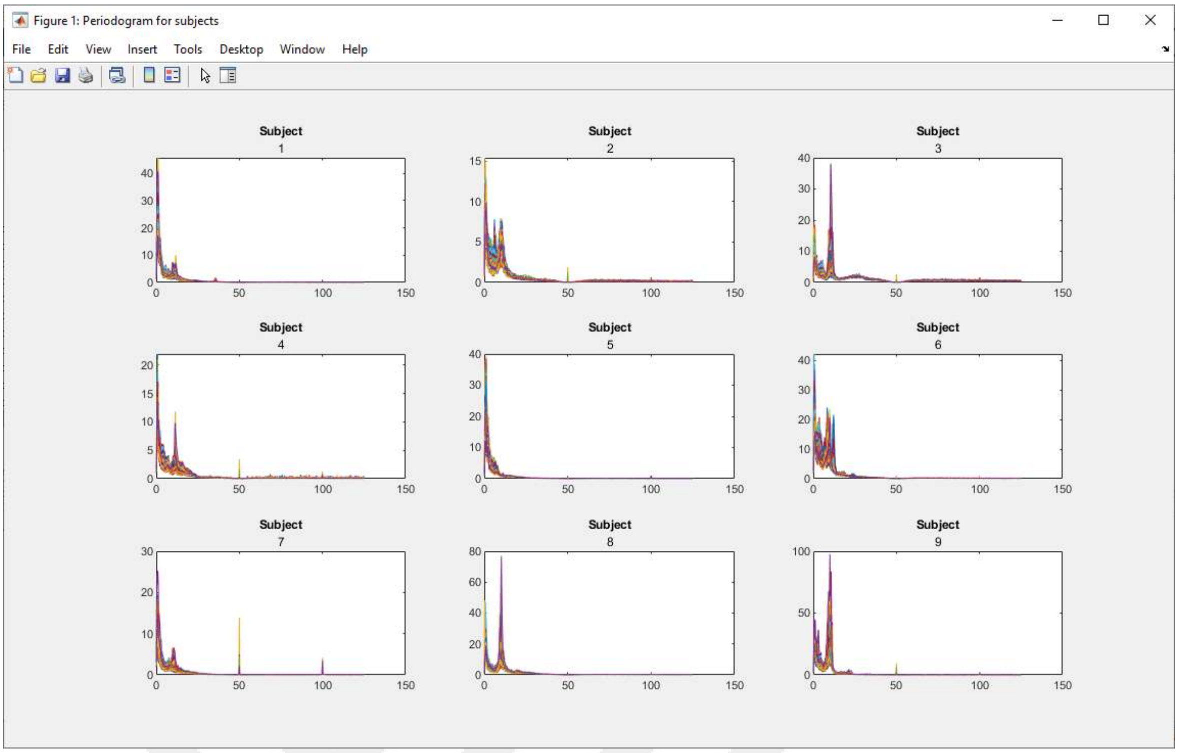

Figure 6. Periodogram for all subjects for all frequency spectrums

After visualizing the power spectrum of signals via periodogram calculations, signals were separated into bands, and brain mapping was done to visualize the electrical activity on electrodes. Figure 14 shows Subject 1's brain mapping of electrodes and electrical activity after periodogram calculation for five bands.

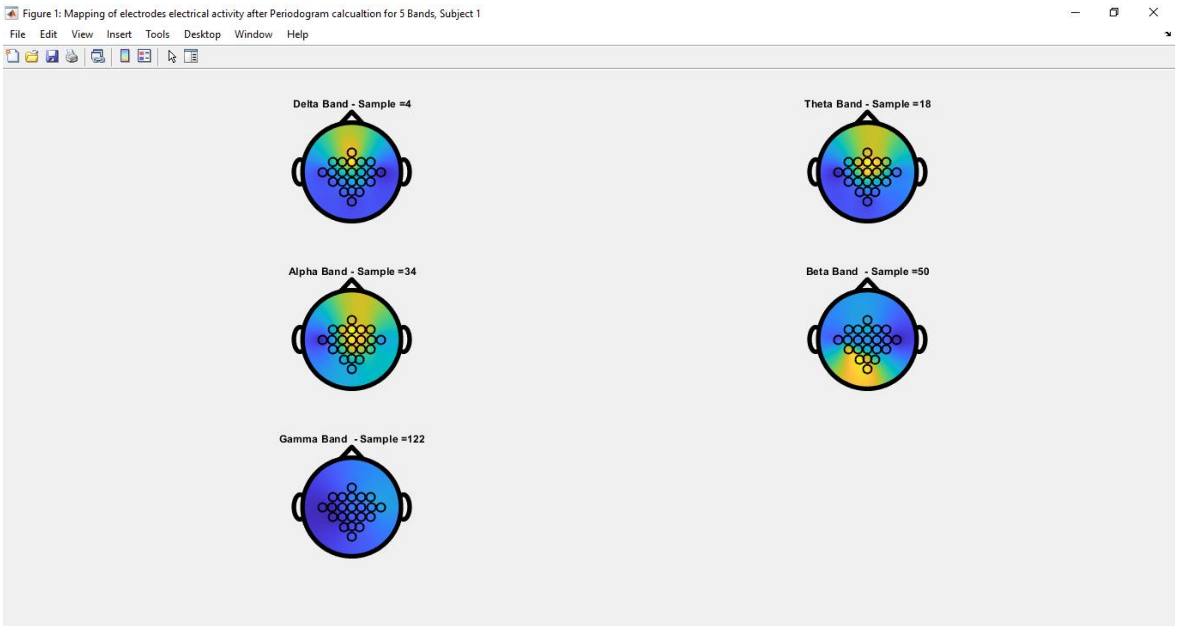

Figure 7. Subject 1- Brain mapping of electrodes and electrical activity after periodogram calculation for 5 bands

3.2.5. Discrete Cosine Transform:

Discrete Cosine Transform (DCT) is one of the powerful feature extraction tools in EEG signal processing. DCT does not directly map to the traditional frequency domain; instead, it provides a compressed representation of the signal's frequency content, focusing on efficiently capturing low-frequency information.

DCT was performed on a 22x22 identity matrix to calculate DCT coefficients. An identity matrix is a diagonal matrix with 1s on the diagonal and 0s elsewhere. The coefficient matrix was multiplied by the subjects' EEG signals.

DCT was performed on electrode signals to reduce neighbor electrodes' electrical activity effect and define the significant features on subjects' EEG signals.

At this stage of the study, DCT was performed on the signals, and the signals were separated into bands. Brain mapping was done to visualize the electrical activity on electrodes for each band individually. Figure 15 shows Subject 1's brain mapping of electrodes and electrical activity after DCT calculation for five bands.

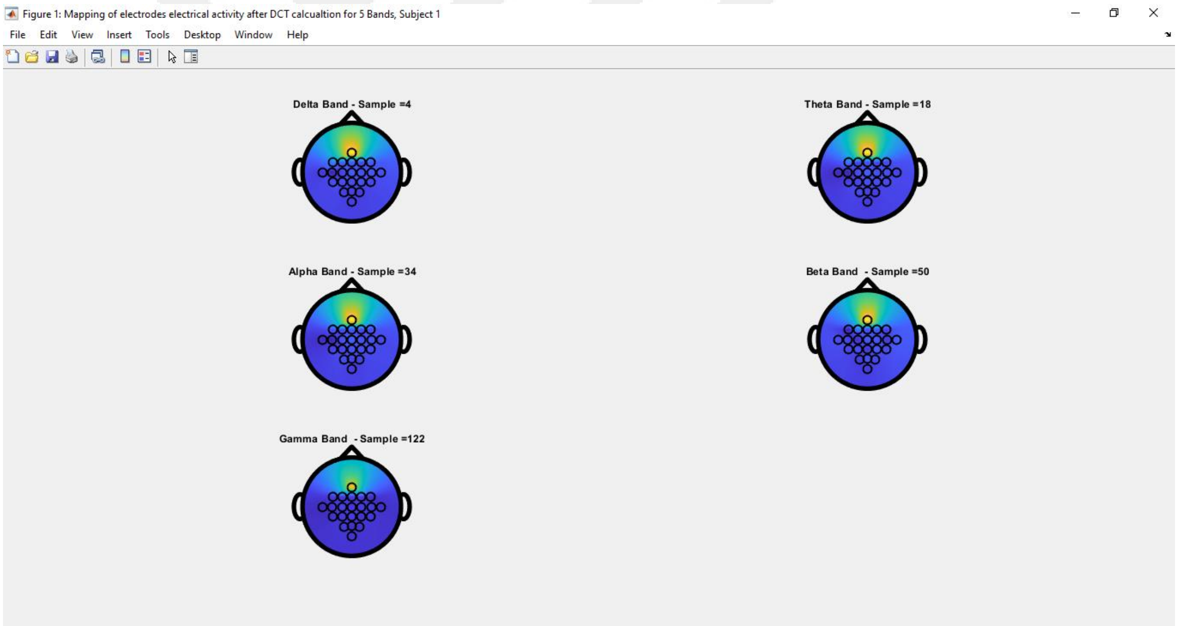

Figure 8. Subject 1- Brain mapping of electrodes and electrical activity after DCT calculation for 5 bands

3.2.6. Reconstruction Independent Component Analysis:

Reconstruction ICA, also known as ICA with reconstruction cost, is a variant of the Independent Component Analysis (ICA) technique used for unsupervised feature learning. rICA introduces a reconstruction cost term into the optimization process. This cost term encourages the learned components not only to be independent but also to contribute to the reconstruction of the original mixed signal. This allows Reconstruction ICA to learn over-complete features and handle unwhitened data more robustly. Reconstruction ICA provides a valuable approach to unsupervised feature learning when dealing with overcomplete features, unwhitened data, or high-dimensional datasets.

At this step, rICA was performed on electrode signals to calculate the weighted matrix. Signals were separated into bands, and brain mapping was done to visualize the electrical activity on electrodes. Figure 16 shows Subject 1's brain mapping of electrodes and electrical activity after Reconstruction ICA calculation for five bands.

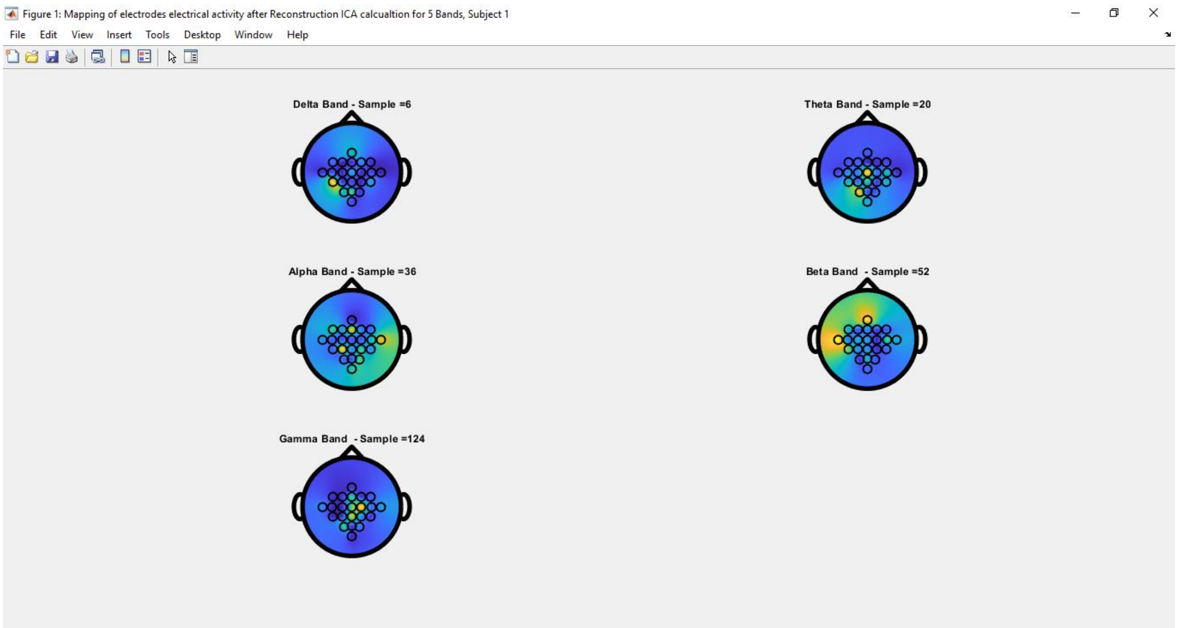

Figure 9. Subject 1- Brain mapping of electrodes and electrical activity after Reconstruction ICA calculation for 5 bands

3.2.7. Comparison of Periodogram, DCT and rICA:

Pre-processed signals in Periodogram, DCT, and rICA feature extraction methods were compared via brain mapping with respect to the electrical activity on electrodes for the Theta, Alpha, and Beta bands.

Figure 17 shows Subject 1's (Left hand) Brain mapping comparison for Periodogram, DCT, and rICA feature extraction methods with respect to the electrical activity on electrodes for the Theta, Alpha, and Beta bands.

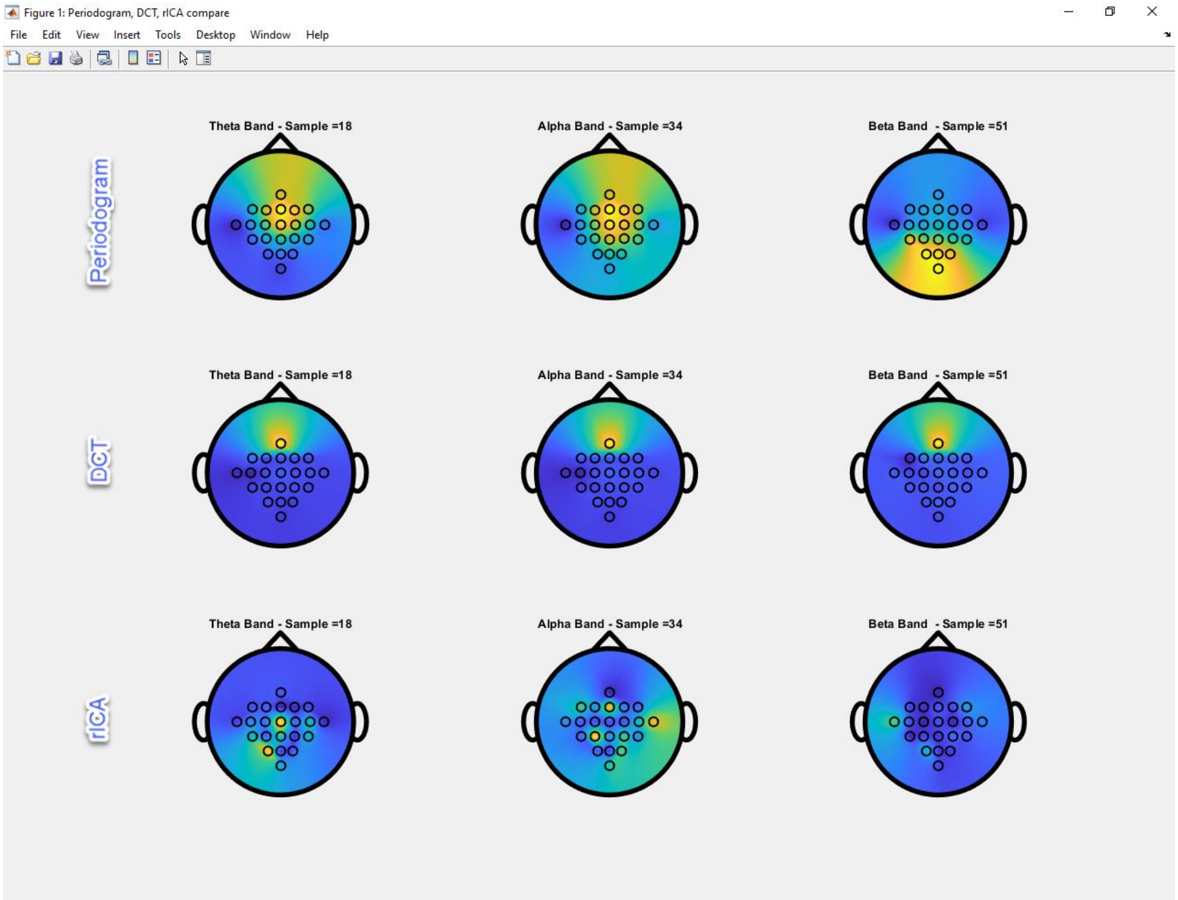

Figure 10. Subject 1- (Left hand) – Brain mapping comparison for Periodogram, DCT and rICA feature extraction methods with respect to the electrical activity on electrodes for Theta, Alpha, Beta bands

There were no distinctive or successful method among the feature extraction functions (Periodogram, DCT, rICA).

3.2.8. Coherence:

Coherence is a method utilized to assess the functional relationship between two distinct brain regions by analyzing their electrical activity. It helps us understand how synchronized these regions are in their oscillatory activity. Coherence focuses on determining the similarity in the frequency content of the signals from two brain regions. This method calculates a value between 0 and 1, where 0 means there is no linear relationship between the frequencies in the two signals, and 1 means perfect coherence, indicating that the signals share identical frequency components.

Coherence offers a frequency-domain approach, which enables researchers to analyze how different brain regions interact at specific frequency bands associated with distinct brain rhythms. This method is a valuable tool in EEG analysis for investigating functional connectivity within the brain. It provides insights into how different brain regions communicate and work together during various tasks and brain states.

At this step of the study, the signals obtained from the EEG electrodes were processed and, the electrodes were correlated with each other (coherence calculated) in terms of skull connectivity, and brain mapping was performed. The results obtained were very close to each other.

The difference between the coherence results of the different classes was calculated and visualized as the next step. It was observed that the results were very close to each other.

The Coherence for all bands and channels was very close to each other, which would prevent successful feature extraction.

3.2.9. Correlation Coefficient and Covariance Matrices Computation:

The correlation coefficient is a statistical measure used to determine the strength and direction of a linear relationship between two variables. It is measured on a scale of -1 to 1, where 1 represents a perfect positive correlation, indicating that as one variable increases, the other increases proportionally. On the other hand, -1 represents a perfect negative correlation, which means that if one variable increases, the other decreases proportionally. A correlation coefficient of 0 indicates that there is no linear relationship between the variables.

When it comes to EEG signal processing, the correlation coefficient is a useful tool in analyzing the relationships between different channels of recorded brain activity. It can be used to extract features from EEG data that may be relevant to classification tasks.

A covariance matrix is a square matrix that captures the covariances between all pairs of features (variables) in a dataset. Covariance indicates how much two features vary together. It represents the tendency of two features to move together. A positive covariance suggests that they increase or decrease together, while a negative covariance indicates that they move in opposite directions. A value close to zero implies little to no linear relationship.

EEG signals are complex and often noisy, making covariance matrices a valuable tool in understanding the relationships between different brain regions. EEG data from multiple electrodes (channels) can be treated as features. The covariance matrix summarizes the covariances between these channels, revealing how different brain areas interact.

The correlation coefficient matrix is preferred when you want a standardized measure of the linear relationship between variables, regardless of their scale. This is often the case in EEG analysis, where the focus is on the strength of the relationships between brain regions rather than the specific voltage values.

The covariance matrix is useful for understanding the raw covariation between variables and their direction of change, where considering the original units might be meaningful.

Correlation coefficient and covariance matrices were computed, and additional feature extraction methods such as mean, standard deviation, and variance were implemented on the computed matrices. New matrices were included in the classification process. The classification methods were "Feed Forward Neural Network (FFNN)," "Naive Bayes Classifier (NBC)," and "Fit

Discriminant Analysis Classifier (LDAC)." Calculations were performed only on the alpha and beta bands of the subjects' recorded EEG signal spectrum. Three seconds of the motor imagery part of the signal was used for the calculations. 0.75 of the data set was used as training data, randomly selected, and 0.25 of the data set was selected for testing purposes.

As the first step in preprocessing the EEG data, Fast Fourier Transformation was used to transform the signals from the time domain to the frequency domain. A 1024-point Discrete Fourier Transform was computed.

The alpha (8-12 Hz) and beta (12-20 Hz) bands were filtered from the transformed signal. The Tukey window function, with r=0.25 cosine fraction, was implemented, and then the data was flipped with respect to the midpoint of the DFT points. The conjugates of the elements in the sequence were calculated. A matrix consisting of the filtered and conjugated samples was created. As the final step of the pre-processing of the EEG data, an inverse fast Fourier transform was performed to obtain a time-domain signal.

The correlation coefficient and the covariance matrices of size 22x22 were computed individually. The covariance matrix was normalized with its sum of diagonals. The upper or lower diagonals were employed as feature vectors. The upper or lower diagonals and main diagonal of the correlation coefficient matrix were employed as features. The diagonal of the correlation coefficient matrix was also excluded.

The flowcharts of the studied method are shown in Figure 18-19.

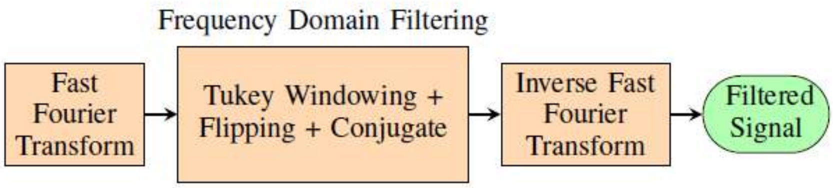

Figure 11. Pre-processing EEG signal

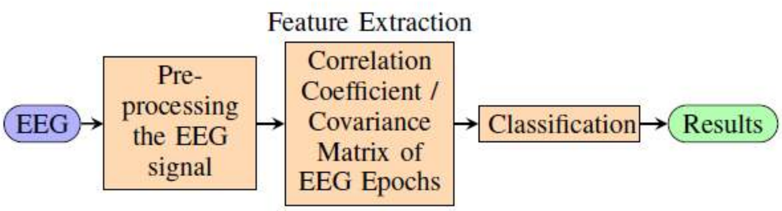

Figure 19. Applied methods

3.2.10. Additionally performed feature extraction methods (Mean, Standard Deviation, Variance, reliefF, PCA):

In addition to the Correlation Coefficient and Covariance matrices, Mean, Standard Deviation, Variance, reliefF, PCA methods were applied to MI data as feature extraction methods.

Every method has been used one by one.

Mean: **mean** function of MatLab (MathWorks) has been used (MathWorks 4, 2024).

Standard Deviation: **std** function of MatLab (MathWorks) has been used (MathWorks 5, 2024).

Variance: **var** function of MatLab (MathWorks) has been used (MathWorks 6, 2024).

reliefF: **relieff** function of MatLab (MathWorks) has been used (Robnik-Šikonja M. and Kononenko I.,2003).

PCA: **pca** function of MatLab (MathWorks) has been used (Jolliffe I. T.,2002).

4. RESULTS AND DISCUSSIONS

At the first stage of this study, the aim was intended to work on scalp connectivity and brain mapping. Thus, periodograms, DCT, rICA, and coherence were used as feature extraction methods before visualization of brain mapping. However there were no distinctive or successful methods among these feature extraction methods. The visual results obtained during brain mapping were not meaningful and interpretable. Therefore, these methods (periodogram, DCT, rICA, and coherence) would not be used in the later stages of the study.

Unsuccessful attempts at brain mapping change the direction of the study from a visual to a computational perspective.

In addition to the Correlation Coefficient and Covariance matrices mean, standard deviation, variance feature extraction methods implemented one by one and obtained data classified with FFNN, NBC, and LDAC classification methods.

Classification results for mean, standard deviation and variance feature extraction methods used in addition to the correlation coefficient and covariance matrices are listed in Tables 1-3.

Table 1. Classification results for featured data (Mean)
Correlation Coefficient– 3 Second 3/4 as training

Subject	FFNN Alpha	NBC Alpha	LDAC Alpha	FFNN Beta	NBC Beta	LDAC Beta
1	47.64	43.06	49.17	40.69	34.72	46.94
2	32.50	32.64	36.53	41.67	29.72	46.53
3	37.22	28.75	46.81	40.83	29.86	50.42
4	32.50	31.11	37.78	32.92	26.39	35.83
5	25.83	28.89	29.03	26.11	23.33	28.61
6	29.58	24.17	33.33	27.08	26.39	27.08
7	34.03	30.83	36.25	41.25	36.25	45.97
8	53.33	40.56	60.00	49.44	34.72	51.53
9	34.44	32.78	38.33	31.81	30.42	34.31
mean	**36.34**	**32.53**	**40.80**	**36.87**	**30.20**	**40.80**

Covariance – 3 Second 3/4 as training

Subject	FFNN Alpha	NBC Alpha	LDAC Alpha	FFNN Beta	NBC Beta	LDAC Beta
1	40.97	30.00	39.86	36.94	23.19	40.83
2	26.67	27.92	33.61	32.78	24.86	39.03
3	47.92	39.58	52.92	30.14	28.33	31.25
4	28.61	30.69	33.47	27.64	29.03	34.31
5	30.14	23.33	30.00	24.58	24.44	29.03
6	30.14	27.50	31.94	26.94	23.47	34.31
7	30.56	30.14	33.75	43.75	28.33	47.92
8	55.00	37.08	57.78	38.19	25.00	47.36
9	30.56	29.72	39.86	38.06	30.42	42.92
mean	**35.62**	**30.66**	**39.24**	**33.23**	**26.34**	**38.55**

Table 2. Classification results for featured data (Standard Deviation)

Correlation Coefficient– 3 Second 3/4 as training

Subject	FFNN Alpha	NBC Alpha	LDAC Alpha	FFNN Beta	NBC Beta	LDAC Beta
1	42.64	42.50	44.31	35.14	33.06	37.08
2	28.89	31.67	31.67	34.44	24.72	38.06
3	39.72	31.81	41.53	34.44	28.06	38.33
4	35.83	32.08	36.39	28.06	27.50	31.11
5	28.75	27.92	30.56	28.75	24.17	28.75
6	25.69	25.97	30.56	25.69	27.36	27.08
7	31.25	32.36	34.44	39.44	36.94	42.64
8	46.53	40.28	50.00	48.61	33.89	47.64
9	29.03	32.78	34.44	30.97	31.11	33.75
mean	**34.26**	**33.04**	**37.10**	**33.95**	**29.65**	**36.05**

Covariance – 3 Second 3/4 as training

Subject	FFNN Alpha	NBC Alpha	LDAC Alpha	FFNN Beta	NBC Beta	LDAC Beta
1	40.56	37.78	41.11	39.72	38.89	37.08
2	25.00	22.78	29.03	38.61	35.42	45.00
3	49.72	37.92	52.50	37.36	39.58	41.81
4	32.78	32.92	36.53	33.06	33.61	38.33
5	28.06	24.86	23.33	29.03	29.44	32.78
6	33.19	27.22	26.25	37.08	36.94	33.19
7	36.81	33.19	34.86	41.81	36.81	48.61
8	56.67	45.83	55.14	38.19	35.69	44.44
9	40.56	39.17	42.22	36.67	39.86	38.61
mean	**38.15**	**33.52**	**37.89**	**36.84**	**36.25**	**39.98**

Table 3. Classification results for featured data (Variance)

Correlation Coefficient– 3 Second 3/4 as training

Subject	FFNN Alpha	NBC Alpha	LDAC Alpha	FFNN Beta	NBC Beta	LDAC Beta
1	40.83	42.64	42.78	34.31	33.47	39.03
2	29.58	28.19	30.83	36.11	23.06	36.25
3	32.22	31.39	34.31	31.67	25.56	39.17
4	33.89	29.17	36.39	27.78	28.47	26.25
5	26.94	27.64	30.28	26.94	24.17	30.97
6	30.14	26.53	31.11	24.72	28.61	25.56
7	35.00	30.42	35.56	37.22	35.28	42.50
8	45.00	38.89	48.61	43.33	35.00	48.89
9	29.72	33.06	32.22	28.89	27.50	28.89
mean	**33.70**	**31.99**	**35.79**	**32.33**	**29.01**	**35.28**

Covariance – 3 Second 3/4 as training

Subject	FFNN Alpha	NBC Alpha	LDAC Alpha	FFNN Beta	NBC Beta	LDAC Beta
1	38.75	35.69	38.47	39.03	34.17	37.36
2	26.67	25.69	28.89	40.69	35.00	39.58
3	42.50	35.83	47.36	38.33	35.28	42.92
4	32.92	29.31	34.31	30.83	30.28	37.36
5	25.42	22.78	25.69	26.67	29.44	31.81
6	29.03	26.39	29.03	31.81	35.00	32.92
7	33.89	32.64	35.28	36.53	33.61	43.47
8	53.61	43.06	50.14	37.92	35.00	39.31
9	41.39	38.89	37.92	36.25	34.31	37.08
mean	**36.02**	**32.25**	**36.34**	**35.34**	**33.56**	**37.98**

Unfortunately, the methods of feature extraction used in the study (Mean, Standard Deviation, Variance) did not result in success to continue working on these methods. The maximum classification accuracy was 40%.

Feature extraction methods, Mean, standard deviation, and variance changed with Relieff, and the same processes were performed as in the previous step.

Classification results for reliefF, in addition to the correlation coefficient and covariance matrices, feature extraction methods are listed in Tables 4-8.

Table 4. Classification results for featured data (ReliefF)-K=20
ReliefF used 3/4 as training (54 of 72 trials) and K=20 for neighbors and for new data matrix with new weighted indexes
Correlation Coefficient– 3 Second 3/4 as training

Subject	FFNN Alpha	NBC Alpha	LDAC Alpha	FFNN Beta	NBC Beta	LDAC Beta
1	39.03	47.22	44.44	27.92	31.94	26.39
2	27.92	29.17	22.22	35.97	37.50	41.67
3	45.28	30.56	41.67	28.47	25.00	37.50
4	26.11	37.50	33.33	24.31	33.33	33.33
5	27.08	37.50	38.89	25.83	26.39	37.50
6	25.69	27.78	26.39	33.89	29.17	31.94
7	31.11	26.39	38.89	32.64	31.94	44.44
8	49.58	34.72	47.22	30.97	25.00	25.00
9	31.25	31.94	41.67	30.83	26.39	37.50
mean	**33.67**	**33.64**	**37.19**	**30.09**	**29.63**	**35.03**

Covariance – 3 Second 3/4 as training

Subject	FFNN Alpha	NBC Alpha	LDAC Alpha	FFNN Beta	NBC Beta	LDAC Beta
1	43.47	25.00	43.06	33.06	33.33	36.11
2	25.14	25.00	19.44	32.78	29.17	34.72
3	46.53	33.33	63.89	30.97	31.94	34.72
4	28.75	29.17	29.17	28.89	22.22	34.72
5	28.19	22.22	29.17	24.86	23.61	27.78
6	28.19	29.17	19.44	29.31	26.39	36.11
7	30.28	30.56	25.00	36.39	23.61	40.28
8	41.81	40.28	65.28	29.03	27.78	31.94
9	35.97	26.39	48.61	29.72	29.17	38.89
mean	**34.26**	**29.01**	**38.12**	**30.56**	**27.47**	**35.03**

Table 5. Classification results for featured data (ReliefF)-K=50

ReliefF used 3/4 as training (54 of 72 trials) and K=50 for neighbors and for new data matrix with new weighted indexes

Correlation Coefficient– 3 Second 3/4 as training

Subject	FFNN Alpha	NBC Alpha	LDAC Alpha	FFNN Beta	NBC Beta	LDAC Beta
1	41.94	38.89	38.89	38.47	29.17	61.11
2	30.00	30.56	44.44	46.25	50.00	38.89
3	43.75	37.50	37.50	44.44	27.78	48.61
4	30.28	26.39	26.39	28.47	36.11	26.39
5	28.33	25.00	34.72	31.81	25.00	36.11
6	25.69	30.56	27.78	30.97	22.22	16.67
7	38.33	37.50	45.83	47.08	26.39	50.00
8	55.42	45.83	58.33	42.08	29.17	48.61
9	39.17	30.56	45.83	41.94	26.39	48.61
mean	**36.99**	**33.64**	**39.97**	**39.06**	**30.25**	**41.67**

Covariance – 3 Second 3/4 as training

Subject	FFNN Alpha	NBC Alpha	LDAC Alpha	FFNN Beta	NBC Beta	LDAC Beta
1	41.53	27.78	45.83	36.81	30.56	56.94
2	25.28	19.44	18.06	45.14	31.94	58.33
3	52.08	37.50	52.78	39.72	33.33	56.94
4	30.69	30.56	25.00	31.53	27.78	36.11
5	29.44	18.06	27.78	27.92	23.61	31.94
6	31.81	23.61	30.56	34.72	29.17	38.89
7	32.92	29.17	47.22	50.83	23.61	63.89
8	55.42	31.94	61.11	38.33	25.00	38.89
9	39.03	27.78	43.06	33.33	29.17	36.11
mean	**37.58**	**27.31**	**39.04**	**37.59**	**28.24**	**46.45**

Table 6. Classification results for featured data (ReliefF)-K1=20,K2=50

ReliefF used 3/4 as training (54 of 72 trials) and K1=20 for neighbors and K2=50 for new data matrix with new weighted indexes

Correlation Coefficient– 3 Second 3/4 as training

Subject	FFNN Alpha	NBC Alpha	LDAC Alpha	FFNN Beta	NBC Beta	LDAC Beta
1	45.69	34.72	55.56	39.03	38.89	55.56
2	32.08	25.00	36.11	45.28	45.83	48.61
3	43.61	40.28	45.83	39.58	30.56	45.83
4	32.64	31.94	30.56	29.72	20.83	38.89
5	33.61	30.56	25.00	31.11	25.00	37.50
6	27.22	30.56	25.00	30.83	23.61	41.67
7	32.92	29.17	37.50	45.42	43.06	51.39
8	59.17	43.06	61.11	39.72	33.33	43.06
9	38.06	29.17	50.00	38.47	23.61	41.67
mean	**38.33**	**32.72**	**40.74**	**37.69**	**31.64**	**44.91**

Covariance – 3 Second 3/4 as training

Subject	FFNN Alpha	NBC Alpha	LDAC Alpha	FFNN Beta	NBC Beta	LDAC Beta
1	42.22	27.78	37.50	35.42	23.61	54.17
2	25.28	22.22	23.61	46.11	37.50	43.06
3	48.61	41.67	55.56	39.44	31.94	40.28
4	32.50	27.78	44.44	32.36	27.78	43.06
5	27.36	27.78	27.78	28.75	26.39	22.22
6	28.33	26.39	23.61	35.83	34.72	37.50
7	35.69	31.94	40.28	52.36	33.33	43.06
8	53.61	37.50	55.56	37.78	25.00	36.11
9	41.81	37.50	40.28	36.53	29.17	34.72
mean	**37.27**	**31.17**	**38.73**	**38.29**	**29.94**	**39.35**

Table 7. Classification results for featured data (ReliefF)-K1=20,K2=100
ReliefF used 3/4 as training (54 of 72 trials) and K1=20 for neighbors and K2=100 for new data matrix with new weighted indexes
Correlation Coefficient– 3 Second 3/4 as training

Subject	FFNN Alpha	NBC Alpha	LDAC Alpha	FFNN Beta	NBC Beta	LDAC Beta
1	40.69	43.06	41.67	43.47	34.72	61.11
2	30.69	37.50	27.78	48.61	43.06	55.56
3	44.44	34.72	38.89	49.58	31.94	44.44
4	31.39	30.56	30.56	33.33	27.78	44.44
5	28.89	33.33	25.00	30.83	36.11	31.94
6	29.86	19.44	36.11	31.25	27.78	33.33
7	38.06	38.89	38.89	47.36	38.89	55.56
8	57.22	59.72	65.28	39.17	37.50	43.06
9	37.50	31.94	48.61	41.67	30.56	37.50
mean	**37.64**	**36.57**	**39.20**	**40.59**	**34.26**	**45.22**

Covariance – 3 Second 3/4 as training

Subject	FFNN Alpha	NBC Alpha	LDAC Alpha	FFNN Beta	NBC Beta	LDAC Beta
1	45.00	23.61	41.67	42.92	20.83	62.50
2	29.58	30.56	22.22	46.39	18.06	43.06
3	60.42	44.44	47.22	40.56	29.17	40.28
4	35.42	25.00	26.39	36.39	29.17	44.44
5	28.61	25.00	27.78	27.92	20.83	31.94
6	32.92	26.39	29.17	34.17	25.00	43.06
7	38.89	33.33	47.22	54.31	25.00	45.83
8	58.89	33.33	62.50	45.97	22.22	44.44
9	44.03	27.78	41.67	37.22	26.39	40.28
mean	**41.53**	**29.94**	**38.43**	**40.65**	**24.07**	**43.98**

Table 8.Classification results for featured data (ReliefF)-K1=20,K2=150

ReliefF used 3/4 as training (54 of 72 trials) and K1=20 for neighbors and K2=150 for new data matrix with new weighted indexes

Correlation Coefficient– 3 Second 3/4 as training

Subject	FFNN Alpha	NBC Alpha	LDAC Alpha	FFNN Beta	NBC Beta	LDAC Beta
1	48.19	40.28	48.61	50.28	36.11	45.83
2	32.78	38.89	31.94	49.86	37.50	55.56
3	52.08	41.67	47.22	55.28	37.50	45.83
4	28.75	41.67	36.11	33.61	23.61	27.78
5	27.08	33.33	25.00	31.11	16.67	18.06
6	33.47	40.28	25.00	32.36	33.33	41.67
7	40.69	33.33	37.50	46.81	41.67	47.22
8	66.81	51.39	52.78	44.31	40.28	36.11
9	38.89	33.33	36.11	40.14	27.78	37.50
mean	**40.97**	**39.35**	**37.81**	**42.64**	**32.72**	**39.51**

Covariance – 3 Second 3/4 as training

Subject	FFNN Alpha	NBC Alpha	LDAC Alpha	FFNN Beta	NBC Beta	LDAC Beta
1	45.69	27.78	38.89	47.78	26.39	50.00
2	29.44	18.06	25.00	51.39	20.83	47.22
3	55.00	36.11	47.22	40.56	23.61	45.83
4	31.81	33.33	25.00	39.31	29.17	31.94
5	31.11	26.39	44.44	28.33	33.33	23.61
6	32.08	27.78	22.22	34.72	25.00	26.39
7	36.53	31.94	41.67	55.42	37.50	50.00
8	62.92	41.67	65.28	46.94	23.61	40.28
9	44.17	31.94	52.78	40.42	34.72	37.50
mean	**40.97**	**30.56**	**40.28**	**42.76**	**28.24**	**39.20**

Unfortunately, the ReliefF method applied as feature extraction in the study did not result in success to continue working on this method. The maximum classification accuracy was %46.45.

The feature extraction method Relieff was replaced with PCA, and the same processes were performed as in the previous step. Only FFNN was used for classification.

Classification results for PCA, in addition to the correlation coefficient and covariance matrices, feature extraction methods are listed in Table 9.

Table 9.Classification results for featured data (PCA)
PCA used 3/4 as training (54 of 72 trials). Highest 10 features selected for process
Correlation Coefficient– 3 Second 3/4 as training

Subject	FFNN Alpha	FFNN Beta	PCA FFNN Alpha	PCA FFNN Beta
1	85.83	86.53	82.22	66.67
2	86.39	87.36	78.33	66.25
3	86.94	87.50	73.89	61.94
4	87.22	86.53	71.67	71.39
5	88.33	87.22	67.50	67.78
6	88.47	87.08	70.28	65.28
7	86.81	87.36	76.53	72.36
8	85.56	86.39	85.00	72.78
9	87.92	87.78	85.97	75.56
mean	**87.05**	**87.08**	**76.82**	**68.89**

Covariance – 3 Second 3/4 as training

Subject	FFNN Alpha	NBC Alpha	LDAC Alpha	FFNN Beta
1	100	100	83.06	81.81
2	100	100	75.42	78.06
3	100	100	87.50	61.67
4	100	100	84.17	84.31
5	100	100	70.83	77.78
6	100	100	89.03	71.39
7	100	100	82.50	79.31
8	100	100	92.08	79.58
9	100	100	85.97	85.42
mean	**100**	**100**	**83.40**	**77.70**

The results for PCA performed on correlation coefficient and covariance matrices compared with correlation coefficient and covariance matrices. The classification accuracy for PCA performed data was %83.40. However, the data for which only correlation coefficients and covariance matrices were calculated have higher classification accuracies. Therefore, it is decided that no additional feature extraction will be performed, and a deep dive will be done on the correlation coefficient and covariance matrices computed data.

Results for Correlation Coefficient and Covariance Matrices Computation as Feature Extraction:

Classification results for Correlation coefficient and covariance matrices feature extraction methods used data listed in Table 10.

Table 10.Classification results for featured data (Correlation coefficient and Covariance matrices)

Correlation Coefficient – 3 Second 3/4 as training

Subject	FFNN Alpha	NBC Alpha	LDAC Alpha	FFNN Beta	NBC Beta	LDAC Beta
1	85.56	55.14	85.14	85.69	39.58	85.28
2	88.33	59.31	83.61	88.47	49.31	85.83
3	86.11	61.67	87.64	88.89	55.69	85.00
4	86.94	67.22	87.22	87.36	45.14	85.14
5	85.97	70.69	84.86	86.53	56.67	87.22
6	85.97	68.61	85.28	86.25	60.28	85.00
7	85.28	61.53	84.86	87.22	40.69	85.97
8	87.92	60.56	86.25	86.94	57.22	87.64
9	86.11	65.00	83.61	86.67	46.25	84.86
mean	**86.47**	**63.30**	**85.39**	**87.11**	**50.09**	**85.77**

Covariance – 3 Second 3/4 as training

Subject	FFNN Alpha	NBC Alpha	LDAC Alpha	FFNN Beta	NBC Beta	LDAC Beta
1	100	100	100	100	97.50	100
2	100	100	100	100	99.72	100
3	100	98.33	100	100	100	100
4	100	99.17	100	100	98.19	100
5	100	100	100	100	100	100
6	100	100	100	100	100	100
7	100	99.58	100	100	95.56	100
8	100	98.89	100	100	98.61	100
9	100	100	100	100	97.50	100
mean	**100**	**99.55**	**100**	**100**	**98.56**	**100**

The class labels were randomly mixed rather than sequential to verify the classification results. The results obtained decreased to almost 0.25, as was expected. These results confirm the accuracy of the classification results.

Classification results for the correlation coefficient and covariance matrices feature extraction methods with mixed class labeled data are listed in Table 11.

Table 11.Classification results for featured data (Correlation coefficient and Covariance matrices)-Mixed class labels

Correlation Coefficient – 3 Second 3/4 as training

Subject	FFNN Alpha	NBC Alpha	LDAC Alpha	FFNN Beta	NBC Beta	LDAC Beta
1	24.86	23.19	28.06	25.83	23.89	24.86
2	25.83	24.17	25.42	21.25	23.19	20.14
3	25.97	25.69	32.08	23.33	25.42	29.44
4	24.58	26.11	22.78	20.97	25.14	21.81
5	22.36	25.00	24.31	26.11	27.64	28.89
6	25.14	25.97	25.14	23.89	29.17	29.03
7	20.83	25.42	22.36	24.72	26.81	25.00
8	25.83	24.31	27.50	25.97	23.19	24.86
9	25.28	23.61	20.14	23.61	23.89	22.08
mean	**24.52**	**24.83**	**25.31**	**23.97**	**25.37**	**25.12**

Covariance – 3 Second 3/4 as training

Subject	FFNN Alpha	NBC Alpha	LDAC Alpha	FFNN Beta	NBC Beta	LDAC Beta
1	24.58	25.42	25.69	25.28	25.42	28.89
2	25.14	29.17	25.14	26.94	29.86	26.11
3	25.56	27.50	29.17	27.08	26.81	23.61
4	22.50	26.25	21.39	23.61	26.39	23.19
5	25.42	28.61	26.11	25.00	24.58	27.08
6	25.28	22.50	20.28	21.94	25.69	20.97
7	22.78	22.50	24.17	21.11	22.08	22.92
8	23.61	23.61	30.56	24.72	22.36	24.86
9	26.39	22.78	23.06	22.08	21.81	24.58
mean	**24.58**	**25.37**	**25.06**	**24.20**	**25.00**	**24.69**

As a result of the studies performed up to now, it was observed that feature extraction processes other than correlation coefficient and covariance matrices were not successful enough. Therefore, in the next stage of the study, only the correlation coefficient and covariance matrices will be used as feature extraction methods. In the processes carried out so far, the computations performed on the 3-second motor imagery part of the EEG data were selected. In the next step, the 1-second data segment (1-second data from 0.5 and 1.5 seconds) will be used, and the correlation coefficient and covariance matrices will be computed for the classification process.

Classification results for the correlation coefficient and covariance matrices feature extraction methods with a 1-second segment of data listed in Tables 12-13.

Table 12.Classification results for featured data (Correlation coefficient and Covariance matrices)-1 second from 0.5

Correlation Coefficient – 1 second segment of data. 3/4 as training

Subject	FFNN Alpha	NBC Alpha	LDAC Alpha	FFNN Beta	NBC Beta	LDAC Beta
1	86.11	69.44	86.11	90.28	56.94	86.11
2	90.28	79.17	86.11	88.89	65.28	84.72
3	91.67	72.22	81.94	88.89	73.61	86.11
4	81.94	72.22	83.33	84.72	70.83	83.33
5	83.33	83.33	84.72	77.78	62.50	81.94
6	84.72	81.94	90.28	84.72	66.67	81.94
7	93.06	76.39	84.72	88.89	54.17	91.67
8	83.33	75.00	83.33	90.28	75.00	88.89
9	84.72	72.22	87.50	87.50	65.28	91.67
mean	**86.57**	**75.77**	**85.34**	**86.88**	**65.59**	**86.27**

Covariance – 1 second segment of data. 3/4 as training

Subject	FFNN Alpha	NBC Alpha	LDAC Alpha	FFNN Beta	NBC Beta	LDAC Beta
1	100	100	100	100	100	100
2	100	100	100	100	100	100
3	100	100	100	100	100	100
4	100	100	100	100	100	100
5	100	100	100	100	100	100
6	100	100	100	100	100	100
7	100	100	100	100	100	100
8	100	100	100	100	100	100
9	100	100	100	100	100	100
mean	**100**	**100**	**100**	**100**	**100**	**100**

Table 13.Classification results for featured data (Correlation coefficient and Covariance matrices)-1 second from 1.5

Correlation Coefficient – 1 second segment of data. 3/4 as training

Subject	FFNN Alpha	NBC Alpha	LDAC Alpha	FFNN Beta	NBC Beta	LDAC Beta
1	81.94	68.06	84.72	86.11	55.56	84.72
2	88.89	76.39	81.94	87.50	61.11	87.50
3	79.17	73.61	81.94	86.11	66.67	88.89
4	88.89	81.94	80.56	88.89	62.50	88.89
5	93.06	73.61	79.17	88.89	70.83	81.94
6	84.72	79.17	88.89	91.67	63.89	86.11
7	91.67	75.00	84.72	87.50	62.50	83.33
8	79.17	77.78	88.89	88.89	52.78	87.50
9	84.72	77.78	84.72	88.89	72.22	88.89
mean	**85.80**	**75.93**	**83.95**	**88.27**	**63.12**	**86.42**

Covariance – 1 second segment of data. 3/4 as training

Subject	FFNN Alpha	NBC Alpha	LDAC Alpha	FFNN Beta	NBC Beta	LDAC Beta
1	100	100	100	100	100	100
2	100	100	100	100	100	100
3	100	100	100	100	100	100
4	100	100	100	100	100	100
5	100	100	100	100	100	100
6	100	100	100	100	100	100
7	100	100	100	100	100	100
8	100	100	100	100	100	100
9	100	100	100	100	100	100
mean	**100**	**100**	**100**	**100**	**100**	**100**

The class labels were randomly mixed rather than sequentially to verify the classification results. The results obtained decreased to almost 0.25, as was expected. These results confirm the accuracy of the classification results.

Classification results for the correlation coefficient and covariance matrices feature extraction methods with mixed class labeled data listed in Tables 14-15.

Table 14.Classification results for featured data (Correlation coefficient and Covariance matrices)-1 second from 0.5-with mixed class labels

Correlation Coefficient – 1 second segment of data. 3/4 as training

Subject	FFNN Alpha	NBC Alpha	LDAC Alpha	FFNN Beta	NBC Beta	LDAC Beta
1	26.11	20.69	23.19	23.61	21.81	28.75
2	23.89	25.14	21.81	23.61	25.83	20.83
3	26.25	25.56	26.25	27.08	25.97	26.53
4	26.25	23.33	23.61	21.39	27.50	20.97
5	22.08	26.81	19.17	23.19	24.17	22.78
6	21.25	21.94	22.36	24.86	21.11	24.44
7	23.75	23.06	19.86	22.64	24.72	27.36
8	22.78	22.64	21.25	25.00	23.33	23.47
9	24.86	22.78	21.81	23.19	25.00	19.31
mean	**24.14**	**23.55**	**22.15**	**23.84**	**24.38**	**23.83**

Covariance – 1 second segment of data. 3/4 as training

Subject	FFNN Alpha	NBC Alpha	LDAC Alpha	FFNN Beta	NBC Beta	LDAC Beta
1	22.78	22.50	20.42	21.25	23.75	23.33
2	22.64	26.81	25.56	24.03	24.17	20.83
3	27.36	33.19	30.69	28.75	33.06	25.14
4	22.92	28.06	24.72	24.44	28.75	23.75
5	26.67	19.03	25.42	23.61	22.22	25.83
6	20.14	22.36	21.11	23.89	23.06	24.72
7	23.33	25.28	22.08	22.50	28.89	28.33
8	22.64	20.56	22.22	23.33	19.72	23.75
9	26.39	22.92	22.78	23.89	28.75	25.28
mean	**23.87**	**24.52**	**23.89**	**23.97**	**25.82**	**24.55**

Table 15.Classification results for featured data (Correlation coefficient and Covariance matrices)-1 second from 1.5-with mixed class labels

Correlation Coefficient – 1 second segment of data. 3/4 as training

Subject	FFNN Alpha	NBC Alpha	LDAC Alpha	FFNN Beta	NBC Beta	LDAC Beta
1	24.03	28.06	25.00	24.44	28.33	26.39
2	22.64	21.81	25.42	25.14	22.50	22.08
3	23.06	18.33	22.92	19.44	22.78	22.78
4	24.44	25.97	26.11	20.83	26.53	26.81
5	25.83	23.75	28.33	22.36	24.86	22.08
6	23.47	24.17	23.61	23.89	27.50	22.92
7	28.19	24.58	23.33	24.17	24.86	30.83
8	22.78	21.67	26.67	24.58	23.33	25.69
9	26.39	31.39	29.17	31.67	26.25	28.61
mean	**24.54**	**24.41**	**25.62**	**24.06**	**25.22**	**25.35**

Covariance – 1 second segment of data. 3/4 as training

Subject	FFNN Alpha	NBC Alpha	LDAC Alpha	FFNN Beta	NBC Beta	LDAC Beta
1	22.92	24.03	24.86	21.53	22.50	24.17
2	22.64	23.75	25.42	18.47	21.11	22.92
3	25.28	17.22	23.06	20.69	20.42	21.39
4	25.83	27.36	29.31	26.25	23.89	25.56
5	25.69	25.83	26.25	21.11	21.94	21.94
6	24.72	21.81	28.06	25.28	19.58	25.97
7	24.44	27.22	24.58	23.47	25.56	23.33
8	22.22	21.81	23.19	23.33	22.92	24.44
9	27.22	30.14	27.78	24.17	29.72	25.00
mean	**24.55**	**24.35**	**25.83**	**22.70**	**23.07**	**23.86**

The success of the classification results obtained so far encouraged us to go one step further. Moreover, the classification result of the selected 1-second segment was shifted by one sample starting from stimuli over 3-second signal (750 samples in total). For each subject and 500 shifts, the classification results were computed (Figure 20). And the average, minimum, and maximum values were calculated.

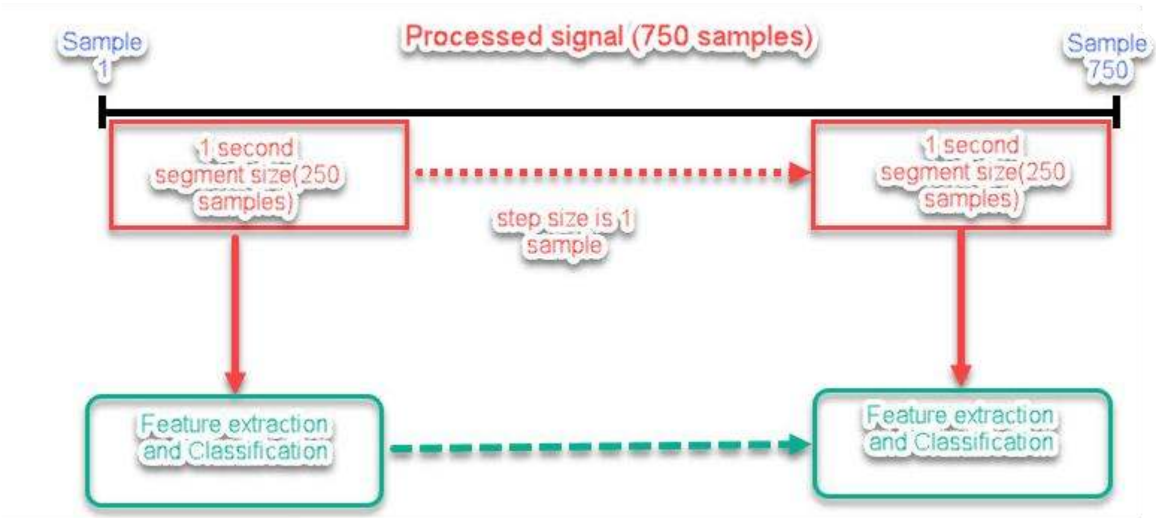

Figure 12. Shifting process of 1 second segment data for 750 samples

As the results were positive, the entire 3-second data (750 samples in total, as the sampling rate was 250 Hz) was analyzed to determine which interval should be selected for the processes. It was observed that balanced results were obtained in the classifications made by applying the "Feed Forward Neural Network" and "Linear Discriminant Analysis Classifier." Since the success calculation was balanced, it was decided that the selection could be made randomly.

The average, minimum, and maximum values of the classification results for shifted 1-second segment data for all subjects are listed in Table 16.

Table 16.The maximum, minimum, and average of classification results for 9 subjects (1 second segment of signal data)

Correlation Coefficient

	FFNN Alpha	NBC Alpha	LDAC Alpha	FFNN Beta	NBC Beta	LDAC Beta
Maximum	96.14	89.81	94.14	96.14	82.72	95.99
Minimum	74.23	62.04	73.15	76.23	43.83	75.31
Average	**86.71**	**76.89**	**84.77**	**87.22**	**64.04**	**85.71**

Covariance

	FFNN Alpha	NBC Alpha	LDAC Alpha	FFNN Beta	NBC Beta	LDAC Beta
Maximum	100	100	100	100	100	100
Minimum	99.84	99.38	99.84	100	96.75	100
Average	**99.99**	**99.99**	**99.99**	**100**	**99.85**	**100**

The study began with a focus on scalp connectivity and brain mapping, employing feature extraction techniques such as periodograms, Discrete Cosine Transform (DCT), reconstruction Independent Component Analysis (rICA), and coherence. The aim was to visualize brain activity. However, these methods failed to produce meaningful or interpretable results. This marks a critical learning point, illustrating that not all commonly used methods are equally effective for every dataset or objective.

Following the unsuccessful attempts at brain mapping, the study shifted from visualization to computational classification.

Mean, Standard Deviation, Variance, ReliefF, PCA feature extraction methods performed one by one on the correlation coefficients and covariance matrices computed data.

Statistical Features Extraction Methods (Mean, Standard Deviation, Variance): These features, combined with classifiers (Feed Forward Neural Network, Naive Bayes Classifier, and Linear Discriminant Analysis), resulted in a maximum accuracy of 40%. This outcome suggests that simple statistical features may not capture the complexity of EEG data for classification tasks.

ReliefF: The implementation of ReliefF, a feature selection algorithm, improved accuracy slightly to 46.45%. While an improvement, this was insufficient to justify its continued use, showing that feature selection alone may not overcome inherent limitations of the features or classifiers used.

PCA (Principal Component Analysis): PCA showed significant promise, achieving 83.40% accuracy when used with FFNN. However, further comparison revealed that raw correlation coefficients and covariance matrices outperformed PCA-processed data. This finding underscores the potential utility of these raw features, suggesting that they might inherently capture the critical patterns required for classification.

The final decision to prioritize correlation coefficients and covariance matrices reflects a data-driven approach. By abandoning less effective methods and focusing on promising features, the study demonstrates methodological rigor and responsiveness to empirical results.

The study illustrates the challenges inherent in EEG data analysis, particularly in identifying appropriate feature extraction methods. Its iterative methodology and flexibility in adjusting the focus are commendable. The finding that raw features like correlation coefficients and covariance matrices outperform advanced techniques like PCA provides valuable insights for similar studies. However, the relatively low performance of many approaches also highlights the difficulty of extracting discriminative information from EEG data, in brain-computer interface (BCI) research.

The final phase focused on analyzing correlation coefficients and covariance matrices, both of which yielded robust classification results:

- Correlation Coefficient Matrix:
    - FFNN and LDAC achieved higher and more balanced classification values for both Alpha and Beta bands.
    - NBC results showed occasional drops, making it less reliable compared to FFNN and LDAC for this feature set.
- Covariance Matrix:
    - FFNN, NBC, and LDAC consistently achieved nearly 100% classification accuracy for both Alpha and Beta bands.
    - Although NBC experienced occasional drops, these did not significantly affect the average accuracy, emphasizing the robustness of covariance-based features.

The study further validated these results by shifting a 1-second data segment (over 500 shifts) within a 3-second signal window. This rigorous evaluation revealed:

- Covariance matrix-based features yielded higher and more homogeneous results across all classifiers compared to correlation coefficients.
- The random selection of any "1-second segment" from the covariance matrix computed data provided consistent classification results for FFNN, NBC, and LDAC, demonstrating the reliability of this feature set.

The superior performance of covariance matrix-based features led to the conclusion that no additional feature extraction methods were necessary. Instead, the study deepened its focus on refining the use of correlation coefficients and covariance matrices for EEG classification.

The main disadvantage of this study was the significant computational time required, which was dependent on the processing power of the computer used. The calculations were performed on a computer with the following specifications: Intel(R) Core(TM) i5-3320M CPU @ 2.60GHz, 64-bit Windows 10 Pro operating system, and 16GB of RAM. To provide an example of the computational time, the creation of the correlation coefficient matrix and the execution of the classification process took a continuous 36 hours process. During this period, no any other processes were running on the computer.

The calculations in this study were performed using MATLAB, a software developed by MathWorks. In the future, to advance this study further, Python, which provides greater computational power, could be utilized.

5. CONCLUSIONS

This study provides a comprehensive exploration of feature extraction and classification methods for EEG signal processing, with a focus on the BCI Competition IV Data Set 2a. Starting with the objective of brain mapping, the study initially attempted techniques such as periodograms, DCT, rICA, and coherence, but these did not yield meaningful or interpretable results. This failure prompted a shift in focus from visual brain mapping to computational classification, a decision that ultimately led to the study's success.

The study systematically tested a range of feature extraction methods, starting with basic statistical features such as mean, standard deviation, and variance in addition to correlation coefficient matrices and covariance matrices. However, these methods resulted in a maximum classification accuracy of just 40%, indicating that they did not adequately capture the complexity of EEG data. Subsequently, the ReliefF feature selection method was applied, improving the accuracy to 46.45%, but still not reaching optimal performance.

Additionally, PCA (Principal Component Analysis) was tested as an alternative feature extraction method and showed a marked improvement in classification accuracy. PCA achieved an accuracy of 83.40% when applied to correlation coefficient and covariance matrix data, further supporting the effectiveness of these basic feature extraction techniques. However, it was found that the raw features themselves (correlation and covariance matrices) led to even higher accuracy, making PCA an unnecessary step in this context.

In a more focused approach, the study investigated correlation coefficient matrices and covariance matrices as feature extraction methods. The results demonstrated that these raw features performed remarkably well, with the covariance matrix achieving nearly 100% accuracy across all classifiers (FFNN, NBC, and LDAC). The correlation coefficient matrix also yielded good results, particularly with FFNN and LDAC, but NBC showed less consistency. Additionally, when a 1-second segment of data was randomly chosen for classification, the covariance matrix features proved to be reliable and robust, further solidifying their utility for EEG classification tasks.

This study sets itself apart from previous research on the same data set by employing these fundamental methods for feature extraction. While other studies used more complex approaches, the simplicity and success of using correlation coefficients and covariance matrices for feature extraction represent a novel contribution. Notably, this is the first study to focus on covariance matrices and correlation coefficient matrices in this context, achieving near-perfect classification accuracy with these basic methods.

The results of this study are impressive when compared to previous work on the same data set. For example, the study by Ting Li et al. (2023) achieved a high accuracy rate of 96.9%. However, this study surpasses previous research by reaching 100% accuracy with covariance matrix feature extraction. The verification results presented in Tables 11, 14, and 15 confirm the effectiveness of this approach.

In conclusion, this study highlights the potential of basic feature extraction techniques like correlation coefficient matrices and covariance matrices for EEG signal processing. By demonstrating that these simple methods can outperform more complex ones, this work offers valuable insights for future research and practical applications, particularly in the area of brain-computer interfaces (BCIs).

Table 17.Studies performed on BCI Competition IV Data set 2a

	Study	Method	Classification Accuracy (%)
1	Qi F. et al ,2021	FBTSCORAL	76.77
2	Badamchizadeh M.A. et al,2018	AR-CSP/LDA	81.33
		CSP/SRSG-FasArt	85.49
3	Yger F., 2013	CSP/SVM	79.17
4	Puthusserypady et al	FBCSP/CNN	68.5
5	Huang S-C. et al, 2023	CSP/SVM	76.82
6	Fang H. et al,2022	FBRTS	77.7
7	Yang L. et al,2022	RCSP/BCM	87.04
8	Gurve D. et al,2019	NCFS/CNN	77.91
9	Xiao Q. et al,2023	OSTFR/3D-CNN	87.24
10	Shenoy H.V. et al,2015	SR-FBCSP/SVM	82.066
11	Li.T. et al,2023	EEG-ARNN	96.9
12	Amin S.U. et al,2020	M-CNN-FM	74.8
13	**Our study**	**Correlation/FFNN**	**86.71**
		Covariance/FFNN	**99.99**
		Correlation/LDAC	**85.81**
		Covariance/LDAC	**100**

REFERENCES

Amin S.U., Muhammad G., Abdul W., Bencherif m., and Alsulaiman M., 2020, MULTI-CNN FEATURE FUSION FOR EFFICIENT EEG CLASSIFICATION,978-1-7281-1485-9/20/c2020 IEEE

Badamchizadeh M.A., Jafarifarmand A., Khanmohammadi S., Nazari M.A., and Tazehkand B.M., June 2018, A New Self-Regulated Neuro-Fuzzy Framework for Classification of EEG Signals in Motor Imagery BCI, IEEE TRANSACTIONS ON FUZZY SYSTEMS, VOL. 26, NO. 3

Berger H., Über das Elektrenkephalogramm des Menschen. Archiv f. Psychiatrie 87, 527–570 (1929). https://doi.org/10.1007/BF01797193

Bertrand, O., Perrin, F. and Pernier, J.,1985, A theoretical justification of the average reference in topographic evoked potential studies, Electroencephalography and Clinical Neurophysiology/Evoked Potentials Section, Volume 62, Issue 6,Pages 462-464,ISSN 0168-5597, https://doi.org/10.1016/0168-5597(85)90058-9

Birvinskas D., Jusas V., Martisius I., Damasevicius R. , 2012, EEG Dataset Reduction and Feature Extraction using Discrete Cosine Transform, 2012 UKSim-AMSS 6th European Modelling Symposium, 978-0-7695-4926-2/12 $26.00 © 2012 IEEE DOI 10.1109/EMS.2012.88

Brunner C., Leeb R., Muller-Putz G. R., Schlogl A., Pfurtscheller G.,2008, “BCI Competition IV Graz data set A”, http://bnci-horizon- 2020.eu/database/data-sets

Cattai T., Colonnese S. Corsi M.C., Bassett D.S., Scarano G., Fallani F.D.C, 2021, Phase/Amplitude Synchronization of Brain Signals During Motor Imagery BCI Tasks, IEEE TRANSACTIONS ON NEURAL SYSTEMS AND REHABILITATION ENGINEERING, VOL. 29, 2021, https://doi.org/10.1109/TNSRE.2021.3088637

Chambers J.A. and Sanei S.,2007, Centre of Digital Signal Processing, Cardiff University, UK, p4-12

Chen, H., Hu, S., Hua, R. et al. ,2021, Improved naive Bayes classification algorithm for traffic risk management. EURASIP J. Adv. Signal Process. (2021). https://doi.org/10.1186/s13634-021-00742-6

Christensen S.M., Holm N.S, Puthusserypady S, An Improved Five Class MI Based BCI Scheme for Drone Control Using Filter Bank CSP, SHYU K.K., HUANG S-C. , TUNG K.J., LEE L., LEE P-L. , AND CHEN Y-H., 2023,Common Spatial Pattern and Riemannian Manifold-Based Real-Time Multiclass Motor Imagery EEG Classification, IEEE Access Digital Object Identifier 10.1109/ACCESS.2023.3340685

Desmedt, J.E., Chalklin, V. and Tomberg, C. Emulation of somatosensory evoked potential (SEP) components with the 3-shell head model and the problem of 'ghost potential fields' when using an average reference in brain mapping. Electroenceph. clin. Neurophysiol., 1990, 77: 243- 258.

Djamal C., Abdullah Y., Renaldi F. (2017),"Brain Computer Interface Game Controlling Using Fast Fourier Transform and Learning Vector Quantization",Journal of Telecommunication, Electronic and Computer Engineering (JTEC), 9(2-5), P71–74.

Fang H. , Jin J. , Ian Daly , and Wang X., JUNE 2022,Feature Extraction Method Based on Filter Banks and Riemannian Tangent Space in Motor-Imagery BCI, IEEE JOURNAL OF BIOMEDICAL AND HEALTH INFORMATICS, VOL. 26, NO. 6

Greenfield L., Geyer D., and Carney P. R.,2012 Reading EEGs: A practical approach. Lippincott Williams and Wilkins,

Gonzalez, R. C., Woods, R. E., 2008. Digital Image Processing (3rd Edition). Pearson, New Jersey, P-954

Gurve D., Delisle-Rodriguez D., Bastos T., and Krishnan S., 2019, Motor Imagery Classification with Covariance Matrices andNon-Negative Matrix Factorization, 978-1-5386-1311-5/19/ c2019 IEEE, P3083-P3086

Hastie T., Tibshirani R. and Friedman J., 2008, The Elements of Statistical Learning, 2nd Edition, NY, Springer, P-745

Hung CI., Lee PL., Wu YT. et al., 2005, Recognition of Motor Imagery Electroencephalography Using Independent Component Analysis and Machine Classifiers. Ann Biomed Eng 33, 1053–1070

Jolliffe I. T.,2002, Principal Component Analysis. 2nd Ed., Springer, P-488

Kendall M.G, 1979. The Advanced Theory Of Statistics, 4th Ed., Macmillan, P-676

Lei Y., Shan H., Jia F., Lin J., 2016, Reconstruction independent component analysis-

based methods for intelligent fault diagnosis, Xi'an Jiaotong University, 978-1-5090-1915-1/16/$31.00 2016 IEEE.

Li C.,Chen M. andLi Z., May 2022, "A Domain Adaptation- Based Method for Classification of Motor Imagery EEG"“Mathematics 2022”

Li K., Sun G., Zhang B., Wu S. and Wu G., 2009,"Correlation Between Forehead EEG and Sensorimotor Area EEG in Motor Imagery Task," Eighth IEEE International Conference on Dependable, Autonomic and Secure Computing, Chengdu, China, 2009, pp. 430-435, doi:10.1109/DASC.2009.66.

Mathworks 1, 2024, https://www.mathworks.com/help/matlab/ref/cov.html, [accessed: 12.05.2024].

Mathworks 2, 2024, https://www.mathworks.com/help/deeplearning/ref/feedforwardnet.html, [accessed: 12.05.2024].

Mathworks 3, 2024, https://www.mathworks.com/help/stats/fitcdiscr.html, and https://www.mathworks.com/help/stats/gmdistribution.html [accessed: 12.05.2024].

Mathworks 4, 2024, https://www.mathworks.com/help/matlab/ref/timeseries.mean.html, [accessed: 07.12.2024].

Mathworks 5, 2024, https://www.mathworks.com/help/matlab/ref/timeseries.std.html, [accessed: 07.12.2024].

Mathworks 6, 2024, https://www.mathworks.com/help/matlab/ref/timeseries.var.html, [accessed: 07.12.2024].

Nayak S.C., Anilkumar C.A., 24 Jul 2023, EEG Normal Waveforms, https://www.ncbi.nlm.nih.gov/books/NBK539805/ [accessed: 07.05.2024].

Neuper C. and Pfurtscheller G.,1996, “post-movement synchronization of beta rhythms in the EEG over the cortical foot area in man,” Neurosci.Lett., vol. 216, pp. 17–20

Nunez, P.L.,1985, Neocortical Dynamics and Human EEG Rhythms. Oxford University Press, New York,

Nunez P. L., Srinivasan R.,2006. Electric Fields of the Brain: The Neurophysics of EEG. Oxford University Press, P640

O. Olabiyi, A. Annamalai, 2012, Analysis and New Implementations of Periodogram-based

Spectrum Sensing, Department of Electrical and Computer Engineering, Prairie View A&M University, 978-1-4673-1466-4/12/$31.00©2012 Crown

Pawan, Dhiman R., 2023, "Electroencephalogram channel selection based on pearson correlation coefficient for motor imagery-brain-computer interface", Measurement: Sensors, 25, art. no. 100616

Qi F., Xiaokun Z., Xiaofeng X., 2021, Correlation Alignment in Filter Bank Riemannian Tangent Space for Motor Imagery Classification, IEEE 3rd International Conference on Frontiers Technology of Information and Computer (ICFTIC)

Rabie R. and Samah R. and Elshahed M., and Ali R.,2015, "Basics of Brain Computer Interface. Intelligent Systems",

Robnik-Šikonja, M., Kononenko, I.,2003, Theoretical and Empirical Analysis of ReliefF and RReliefF. Machine Learning 53, 23–69, 2003 Kluwer Academic Publishers. https://doi.org/10.1023/A:1025667309714

Sharma V., Aug 2020, Brain Computer Interface, International Journal of Engineering and Advanced Technology (IJEAT) ISSN: 2249-8958 (Online), Volume-9 Issue-6

Shenoy H.V., Vinod A.P., Guan C.,2015, Shrinkage Estimator Based Regularization for EEG Motor Imagery Classification, 978-1-4673-7218-3/15/ c2015 IEEE, ICICS 2015

Schneider M., Broggini A.C., Dann B., Tzanou A., Uran C., Sheshadri S., Scherberger H., Vinck M., 2021, A mechanism for inter-areal coherence through communication based on connectivity and oscillatory power, Neuron 109, 4050–4067, December 15, 2021

Subasi, A. (2019). “Feature extraction and dimension reduction,” in Practical Guide for Biomedical Signals Analysis Using Machine Learning Techniques, ed A. Subasi (San Diego, CA: Elsevier), 193–275. doi: 10.1016/B978-0-12-817444-9.00004-0

Sun B., Liu Z., Wu Z., Mu C., and Li T., SEP 2023, Graph Convolution Neural Network Based End-to-End Channel Selection and Classification for Motor Imagery Brain–Computer Interfaces, IEEE TRANSACTIONS ON INDUSTRIAL INFORMATICS, VOL. 19, NO.9

Tortora, G.J.; Derrickson, B. “Principles of anatomy and physiology”. 13.ed. New York: John Wiley & Sons, 2011.

Xiao Q., Shen J., Chang L., Jia S.,2023, Optimized Spatio-temporal Feature Representation Based on 3D-CNN Motor Image Decoding, 2023 6th International Conference on Computer Network, Electronic and Automation (ICCNEA)

Yang L., Niu X., Zhang X., 2022, MI-EEG Recognition Based on Euclidean Alignment and Style Transfer Mapping, 2022 2nd International Conference on Computational Modeling, Simulation and Data Analysis (CMSDA)

Yger F., SEP 2013, A Review of Kernels on Covariance Matrices For Bci Applications, 2013 Ieee International Workshop On Machine Learning For Signal Processing, Southampton, Uk

Zhiqiang S., Hongchu C., Yanping C., 2012, Application of periodogram and Welch based spectral estimation to vortex frequency extraction, School of Energy Science and Engineering, Central South University,978-0-7695-4608-7/11 $26.00 © 2011 IEEE, DOI 10.1109/ISdea.2011.312

Zhou J., Chen P., 2009, Generalized discrete cosine transform, 2009 Pacific-Asia Conference on Circuits, Communications and System

CURRICULUM VITAE

Salih MENDİ, completed his primary, middle, and high school education in Midyat, Mardin. In 2009, he graduated from Çukurova University, Faculty of Engineering and Architecture, Department of Electrical and Electronics Engineering, which he began in 2003. He started his Master's program at Çukurova University, Institute of Natural and Applied Sciences, Department of Electrical and Electronics Engineering in 2022 and is currently continuing his Master's studies. In 2005, he worked as an officer at Çukurova University Rectorate, Administrative and Financial Affairs Department. In 2012, he left his position at the university and transitioned to the private sector. He is currently working for a private company in the healthcare industry.